Title

TRAIP plays an essential role in the dissociation of PCNA from chromatin during mitosis

Author

Yasushi Shiomi[1,*], Asuka Tadokoro[1], Yuichiro Saito[2,†], Masato T. Kanemaki[2,3,4], Hideo Nishitani[1]

[1]Graduate School of Science, University of Hyogo, Kamigori, Ako-gun, Hyogo, 678-1297, Japan.

[2]Department of Chromosome Science, National Institute of Genetics, Research Organization of Information and Systems (ROIS), Yata 1111, Mishima, Shizuoka, 411-8540, Japan.

[3]Department of Advanced Studies, The Graduate University for Advanced Studies (SOKENDAI), Yata 1111, Mishima, Shizuoka, 411-8540, Japan

[4]Department of Biological Science, The University of Tokyo, Tokyo, 113-0033, Japan

*Correspondence: shiomi@sci.u-hyogo.ac.jp

[†]Current address: Molecular Biology Program, Memorial Sloan Kettering Cancer Center, New York, NY 10065, USA

Abstract

Loading PCNA onto chromatin is a pivotal step in DNA replication, cell cycle progression, and genome integrity. Conversely, unloading of PCNA from chromatin is a crucial step for the maintenance of genome stability. Cells defect of the PCNA unloader ATAD5/Elg1-RFC exhibit a high level of chromatin-bound PCNA, delayed S phase progression, abnormal association/dissociation of chromatin-bound proteins, and aberrant chromosome structures, but exhibit dissociation of PCNA

from chromatin in mitosis. Here, we found that TRAIP, an E3 ubiquitin ligase, plays critical roles in the removal of PCNA from chromatin during mitosis. TRAIP-depleted cells exhibited chromatin-bound PCNA even during mitosis and delayed mitotic progression and mitotic exit. Although TRAIP-depleted cells with chromatin-bound PCNA progressed into the next G1 phase, they showed reduced levels of the replication licensing factor Cdt1 and impaired S phase entry. These results demonstrate that TRAIP functions independently of ATAD5/Elg1-RFC for the removal of PCNA from chromatin during mitosis, and is required for precise cell cycle progression from mitosis to G1 phase, as well as for pre-RC formation for faithful initiation of DNA replication.

Key words

Replication/cell cycle/ubiquitination/

Introduction

Genomic information is maintained by accurate replication and chromosome segregation during S phase and mitosis, respectively. For DNA replication initiation, origins are licensed between the end of mitosis and the beginning of G1 phase through the formation of a pre-replication complex (pre-RC). This is conducted by loading the MCM2-7 complex onto ORC-bound origin with the aid of Cdc6 and Cdt1. At the onset of S phase, replication origins are activated by CDK and DDK, resulting in the loading of a complex composed of the DNA helicase MCM2-7, GINS, and Cdc45, called CMG (Cdc45-MCM2-7-GINS) (Nishitani and Lygerou 2004; Masai et al. 2010; Costa and Diffley 2022). After origin unwinding, polymerase (Pol) α/primase synthesizes primers on both strands, and then Pol ε and Pol δ synthesis the leading and lagging strands, respectively. For these Pols to synthesize new strands processively and stably, they are tethered to the sliding clamp PCNA. After primer synthesis,

PCNA is loaded onto the 3' end of the primer by a protein complex termed the clamp loader, replication factor C (RFC) complex. PCNA is required not only for DNA replication itself, but also for replication-linked processes, such as chromatin assembly and remodeling, epigenetic inheritance, and sister-chromatid cohesion, via its ability to recruit and orchestrate crucial players (Waga and Stillman 1998; Kelch et al. 2012; Burgers and Kunkel 2017).

An authentic RFC1-RFC complex binds PCNA, opens its ring structure, and loads it at the 3' terminus of the primer in an ATPase-dependent manner. In addition to RFC1-RFC, eukaryotic cells possess other PCNA-associating RFC-like complexes, termed Ctf18-RFC and ATAD5-RFC, which contain Ctf18 and ATAD5 (also known as Elg1 in yeast), respectively, instead of canonical RFC1, and the common RFC2-5 small subunits. Ctf18-RFC also has two additional subunits, Ctf8 and Dcc1, that are required for the establishment of sister-chromatid cohesion. Loss of ATAD5/Elg1 results in genome instability, but its precise role was unknown (Shiomi and Nishitani 2017; Ohashi and Tsurimoto 2017).

Since cells have three different PCNA-associating RFC complexes, previously we performed RNAi knockdown of the large subunits of these complexes to determine their roles in cell cycle progression and genomic stability. The results revealed that ATAD5/Elg1 depletion caused large accumulation of PCNA on chromatin during S phase and even the retention of PCNA on chromatin during G2 phase. We also reported that ATAD5/Elg1 depleted cells exhibited various other abnormalities, including S phase progression delay, unusual assembly or disassembly of chromatin-bound proteins, extended chromatin loop structures in inter-phase, and chromosome aberrations such as breaks and lagging-strand chromosomes during mitosis (Shiomi and Nishitani 2013). Studies by our and other groups clearly demonstrated that in contrast to other RFC complexes, ATAD5/Elg1-RFC plays an important role in the maintenance of genomic stability by regulating PCNA unloading from chromatin (Lee et al. 2013; Kubota et al. 2013; Shiomi and Nishitani 2013). During the course of these

studies, we noticed that PCNA dissociated from chromatin in cells arrested at mitosis even when they were depleted of ATAD5/Elg1 (Shiomi and Nishitani 2013), suggesting that cells possess additional unloader(s)/remover(s) of PCNA from chromatin.

When DNA synthesis during replication is terminated, the key regulated step that induces CMG disassembly from chromatin is ubiquitination of the MCM7 subunit of the MCM2-7 complex (Maric et al. 2014; Moreno et al. 2014). Poly-ubiquitinated MCM7 is removed from chromatin by the AAA+ ATPase chaperon p97 (also known as valosin-containing protein (VCP) or Cdc48) (Maric et al. 2017; Deegan et al. 2020). *S. cerevisiae* studies revealed that p97/VCP unfolds poly-ubiquitinated MCM7 and dissociates the CMG complex in an irreversible manner into CDC45, GINS, and subcomplexes of MCM2-7 (Mukherjee and Labib 2019; Deegan et al. 2020).

E3 ubiquitin ligases, which ubiquitinate MCM7, are required for CMG disassembly. The cullin ligase SCF-Dia2 in *S. cerevisiae* (Maric et al. 2017) and CUL2-LRR1 (Merlet et al. 2010; Burger et al. 2013) in *C. elegans* (Sonneville et al. 2017) and *X. laevis* (Dewar et al. 2017; Sonneville et al. 2017) ubiquitinate MCM7 when DNA synthesis terminates during S phase. Studies of *C. elegans* CUL2-LRR-1 also revealed the existence of a second factor for CMG disassembly from chromatin that had not previously been observed in budding yeast. When LRR-1 was depleted, CMG remained on chromatin after DNA replication termination, but dissociated after entry into mitosis (Sonneville et al. 2017). This was also observed when *Xenopus* egg extracts lacking CUL2-LRR1 were driven into mitosis by premature activation of CDK (Deng et al. 2019; Priego Moreno et al. 2019). In both studies, mitotic CMG disassembly required a metazoan-specific RING ubiquitin ligase known as TRUL-1 in *C. elegans* (TRAIP Ubiquitin Ligase 1) and TRAIP in vertebrates (Deng et al. 2019; Priego Moreno et al. 2019; Sonneville et al. 2019).

TRAIP is a nuclear protein required for genome integrity in mammalian cells. TRAIP is

recruited to sites of DNA damage by binding to PCNA via its PCNA interacting peptide sequence (PIP box) located at its C terminal end. It also ensures effective DNA damage signaling and repair by interacting with several repair factors associated with the DNA damage response (Chapard et al. 2014; Wallace et al. 2014; Harley et al. 2016; Hoffmann et al. 2016; Soo Lee et al. 2016; Han et al. 2019; Li et al. 2020).

Human TRAIP has been proposed to be involved in the processing of stalled replication forks based on reports showing defects in fork recovery after the induction of specific forms of DNA damage in cells lacking TRAIP activity (Harley et al. 2016; Hoffmann et al. 2016). Moreover, recent reports indicate that TRAIP is required for mitotic processing of sites of incomplete DNA replication in human cells to preserve genome integrity (Sonneville et al. 2019). Under normal cell cycle conditions, two ubiquitin ligases have been reported to mediate the dissociation of CMG from chromatin, CRL2-LRR1 during S phase and TRAIP during mitosis(Villa et al., 2021) in CRL2-LRR1 defective cells (Villa et al. 2021). Although the PIP box of TRAIP is clearly required for the effectiveness of the DNA damage response, it remains to be elucidated why it is not required for MCM7 ubiquitination, a prerequisite for MCM7 dissociation from chromatin (Villa et al. 2021).

Here, we report that TRAIP plays an essential role in the removal of PCNA from chromatin during mitosis via its PIP box. The expression levels of TRAIP increased after onset of S phase, and peaked between late S phase and mitosis. Additionally, GFP-tagged TRAIP co-localized with PCNA in a PIP box-dependent manner. Stable co-localization between TRAIP and PCNA required CDK1 activity. TRAIP-depleted cells showed retention of PCNA on chromatin throughout mitosis and a delay the mitotic progression and exit. Eventually, however, cell progressed into the next G1 phase despite the presence of chromatin-bound PCNA. The persistence of chromatin-bound PCNA triggered Cdt1 degradation and blocked pre-RC formation. These results demonstrate that in contrast to

ATAD5/Elg1-RFC, which functions during S phase, TRAIP is essential for precise cell cycle progression and the maintenance of genome stability through its ability to regulate the clearance of PCNA from chromatin during mitosis.

Results

TRAIP and p97/VCP mediated dissociation of PCNA from chromatin during mitosis

Previously, we reported that ATAD5/Elg1-depleted human cells show elevated levels of chromatin-bound PCNA, indicating that ATAD5/Elg1-RFC is important for the unloading of PCNA from chromatin. Interestingly, however, PCNA dissociated from chromatin in those cells when they were arrested in mitosis by nocodazole, indicating that the cell possesses another mechanism for the removal of PCNA from chromatin (Shiomi and Nishitani 2013). These results were confirmed using HCT116 cells expressing N-terminus mAID-tagged ATAD5/Elg1 (Fig 1A). The level of chromatin-bound PCNA in these cells collected 72 hours after auxin (IAA) treatment was 2-fold higher in asynchronous cells than in control cells, but decreased in mitotic-arrested cells. It should be noted that the levels of chromatin-bound PCNA in asynchronous cells were equal to those in S phase cells, because PCNA binds to chromatin only during S phase during normal cell cycle progression.

CMG complexes comprising MCM2-7, which are essential for DNA replication initiation, are removed from chromatin by E3 ubiquitin ligases CRL2-LRR1 and TRAIP, which ubiquitinate MCM7 during S phase and mitosis, respectively, during normal cell cycle progression (Maric et al. 2014; Dewar et al. 2017; Priego Moreno et al. 2019; Villa et al. 2021). Curiously, TRAIP has a PIP box at its C-terminus, but it is not required for the ubiquitination of MCM7 during mitosis (Villa et al. 2021). However, we cannot rule out the possibility that TRAIP associates and ubiquitinates PCNA via its PIP box, because PCNA is retained on chromatin in mitotic-arrested cells after the addition of

T2AA, an inhibitor of interactions between PCNA and PIP box-containing proteins (Punchihewa et al. 2012) (Fig1A). Thus, we first monitored the level of PCNA in the chromatin-bound fraction during mitosis after depleting p97/VCP, which recognizes and dissociates poly-ubiquitinated proteins from chromatin (Fig1B). In asynchronous cells, although the levels of PCNA in the chromatin fraction were not different between control and p97/VCP-depleted cells, the level of MCM2 was increased in the chromatin fraction of p97/VCP-depleted cells, indicating that CMG was removed from chromatin by the ubiquitination system including p97/VCP during S phase. In cells arrested at mitosis, the level of chromatin-bound MCM2 was higher in p97/VCP-depleted cells than in control cells, demonstrating that CMG was removed from chromatin by the ubiquitination system both in S phase and mitosis. On the other hand, PCNA remained bound to chromatin in p97/VCP-depleted cells arrested at mitosis, indicating that not only CMG but also PCNA are removed from chromatin by the ubiquitination system during mitosis. After long exposure of PCNA immunoblots of p97/VCP-depleted cell samples, faint and smeared bands appeared at molecular weight positions that were higher than those of the PCNA monomer, indicating that poly-ubiquitinated PCNA was retained on chromatin after depletion of p97/VCP (Fig 1C). Depletion of TRAIP resulted in a reduction of chromatin-bound MCM2 when cells were arrested at mitosis, similar to what was observed in control cells, indicating that CMG was dissociated from chromatin by CRL2-LRR1 during S phase progression even in the absence of TRAIP (Fig1D). Conversely, PCNA was retained in the chromatin-bound fraction of TRAIP-depleted cells even during mitosis, demonstrating that TRAIP was required for the removal of PCNA from chromatin during mitosis. Additionally, the level of chromatin-bound PCNA increased during mitosis after depletion of both ATAD5/Elg1 and TRAIP, indicating that both ATAD5/Elg1 and TRAIP were required sequentially for the removal of PCNA from chromatin throughout cell cycle progression (Fig S1). It should be noted that CRL2-LRR1 was not involved in the removal of PCNA from chromatin during mitosis (Fig EV1 and EV2). When we depleted LRR1 from cells, MCM2 dissociated from

chromatin during mitosis, because TRAIP can serve as a substitute for LRR1 for the ubiquitination of MCM7 during mitosis, as reported previously (Villa et al. 2021). In LRR1-deleted cells, PCNA was also removed from chromatin in mitotic-arrested cells, as observed in control cells. Together, these results demonstrated that TRAIP and p97/VCP, via their poly-ubiquitination and chaperon functions, respectively, constitute a novel pathway for the removal of PCNA during mitosis.

PCNA-K164 is required for the removal of PCNA from chromatin during mitosis

To test the requirement for poly-ubiqitination in the removal the PCNA from chromatin during mitosis, we transfected cells with 6myc-tagged PCNA-WT or -K164R, and monitored their levels in chromatin-bound fractions (Fig 1E). The lysine at position 164 (K164) in PCNA is known to be mono- and poly- ubiquitinated by Rad18 and Rad5 during the DNA damage response and template switching (Hoege et al. 2002; Stelter and Ulrich 2003), and CRL4-Cdt2 mono-ubiquitinates PCNA to promote translesion DNA synthesis in undisturbed cells (Terai et al. 2010). In yeast, SUMOlyration of K164 occurs prior to ubiqitination during the DNA damage response (Papouli et al. 2005; Pfander et al. 2005). WT or K164R PCNA tagged with 6myc was expressed transiently in cells at equal protein levels (Fig 1E, A, and M of whole cell extract (WCE)). When these cells were arrested during mitosis, 6myc-PCNA-WT disappeared from the chromatin-bound fraction, but 6myc-PCNA-K164 did not, while endogenous PCNA was dissociated from chromatin in both cells (Fig 1E, A, and M of Chr), demonstrating that poly-ubiquitination at K164 is required for the removal of PCNA from chromatin during mitosis. Collectively, the results suggest that PCNA is removed from chromatin during mitosis by the p97/VCP chaperon after poly-ubiquitination at K164 by TRAIP.

TRAIP expression increases during S phase and associates with PCNA

To understand the mechanism responsible for the removal of PCNA from chromatin during

mitosis by TRAIP, we first examined the expression levels of endogenous TRAIP protein during cell cycle progression (Fig 2A). U2OS cells arrested at G1/S phase with a thymidine block were released into S phase and collected at the indicated times. Cells arrested at mitosis and G1 phase by the addition of nocodazole (Noco) and lovastatin (lova), respectively, were also collected. An examination of the level of chromatin-bound PCNA demonstrated that PCNA bound to chromatin during S phase (Thy to 8h) and dissociated from chromatin at the end of S phase (around 10h), mitosis, and G1 phase. The TRAIP protein level gradually increased after onset of S phase, peaked during late S phase, consistent with what was reported previously (Chapard, Hohl and Huber 2015), and then decreased at G1 phase. Conversely, the ATAD5/Elg1 protein level peaked at middle S phase, indicating that its expression was regulated slightly differently from that of TRAIP (Fig EV3).

To study TRAIP expression during normal cell cycle progression in more detail, we established U2OS cells ectopically expressing WT TRAIP tagged at its N-terminus with GFP (GFP-TRAIP) (Fig 2B). The expression levels of GFP-TRAIP was equal to that of endogenous TRAIP (Fig 2C). We first examined the association between GFP signals and immunofluorescence signals for Cdt1, Cyclin A, and cyclin B, which are expressed specifically during G1, S and G2 phase, respectively (Fig 2D). Approximately 58.7% and 73.0% of GFP-TRAIP was co-expressed with Cyclin A and Cyclin B, respectively, indicating that GFP-TRAIP expression increased after onset of S phase and continued to increase until mitosis, consistent with the result shown in Fig 2A. Conversely, 14.0% of GFP-TRAIP was co-expressed with Cdt1, suggesting that TRAIP was degraded by the proteasome system during G1 phase, consistent with the result obtained with endogenous TRAIP (Fig 2A). Next, we examined the expression of TRAIP during S phase in more detail in GFP-TRAIP expressing cells. GFP-TRAIP cells were arrested at G1/S phase with thymidine, and then released into S phase and collected at indicated times for fluorescence monitoring (Fig 2E). GFP-TRAIP expression gradually increased with the progression of S phase, and the ratios of its expression per nucleus ranged from approximately

30% at early S phase to approximately 80% at late S phase, as observed before for endogenous TRAIP expression (Fig 2A). Since GFP-TRAIP sometimes exhibits a dot staining pattern resembling PCNA foci during S phase, we examined the co-localization of GFP-TRAIP fluorescence with immunofluorescent PCNA (Fig 2F). PCNA forms foci after the onset of S phase, and the number of these foci changes drastically during progression of S phase (Celis and Celis 1985; Chagin et al. 2016). We pre-extracted cells with detergent before cell fixation to release chromatin-unbound proteins. During G1 phase, GFP-TRAIP signals were hardly detected in the nucleus, suggesting that almost all GFP-TRAIP had been proteolyzed at this stage by the ubiquitination system, as shown in Fig 2A and 2D. In early S phase, PCNA formed large numbers of small foci, while GFP-TRAIP was detected evenly throughout the whole nucleus without foci formation (Fig 2F, early S). In middle S phase, GFP-TRAIP formed small foci and some of its foci co-localized with PCNA. In late S phase, GFP-TRAIP formed large foci and almost all GFP-TRAIP co-localized with PCNA, suggesting that they interacted together. The interaction between GFP-TRAIP and PCNA was robust, because co-localization persisted even after pre-extract treatment. These results demonstrated that TRAIP interacted with chromatin-bound PCNA from middle to late S phase, concomitantly with the increase in the level of TRAIP protein during S phase.

PIP box of TRAIP was required for its interaction with PCNA and removal of PCNA from chromatin

TRAIP contains a PIP box at its C-terminus end, strongly suggesting that the PIP box mediates its interaction with PCNA. To confirm this, we generated two PIP mutants of GFP-TRAIP (Fig 2B): one with phenylalanine (F) at position 466 substituted with alanine (A) in (mPIP)and one with an entire deletion of the PIP box (from glutamine (Q) at 460 to serine (S) at 469) (ΔPIP) (Hoffmann et al. 2016). The expression levels of WT TRAIP and its two derivatives mutants were the

same and equal to that of endogenous TRAIP (Fig 2C). Both PIP box mutants exhibited the same expression pattern as WT TRAIP during cell cycle progression, and their GFP signals increased during late S phase (Fig 3A). These mutants, however, did not form foci even in late S phase, and in contrast to WT TRAIP, they were mostly lost from nuclei by pre-extract treatment of cells 9 hours after release from thymidine arrest (Fig 3B). These results demonstrated that the PIP box of TRAIP was required for its interaction with PCNA during middle to late S phase, and that at least F at position 466 is critical for its binding to PCNA. To confirm that the PIP box was required for the release of PCNA from chromatin, we examined the level of chromatin-bound PCNA in the GFP-TRAIP PIP deletion mutants arrested at mitosis (Fig 3C). The chromatin-bound protein levels of MCM5 and PCNA in GFP-TRAIP (WT) cells were the same as those in control cells, indicating that ectopically expressed GFP-TRAIP (WT) did not disturb the release of chromatin-bound PCNA during mitosis. In GFP-TRAIP (ΔPIP) expressing cells arrested in mitosis, PCNA was retained on chromatin, whereas MCM5 was released because the CRL2-LRR1 removed CMG from chromatin before entry into mitosis (Villa et al. 2021) (Fig 3C). These results clearly demonstrated that the PIP box of TRAIP was required not only for binding to PCNA but also for the release of PCNA from chromatin during mitosis.

TRAIP phosphorylation was required for its stabilization and association with PCNA

We noticed that TRAIP bands were slightly retarded in immunoblots when cells were arrested in mitosis with nocodazole, suggesting that TRAIP might be phosphorylated during early mitosis by CDK1 (Fig 2A, compare 10h, Noco, and Lova). To test whether TRAIP phosphorylation is required for its activity, the CDK1 inhibitor RO3306 was added to GFP-TRAIP expressing cells 1 hour after their release from G1/S arrest with thymidine, and the cells were collected 8 hours after RO3306 treatment (Fig 3D). When the cells approached late S phase, the nuclear expression of GFP-TRAIP was higher (about 46%) than that of cells arrested at G1/S phase (about 20%). However, after

the addition of RO3306, GFP-TRAIP expression was clearly reduced (about 26%). Additionally, RO3306 inhibited the formation of TRAIP foci during late S phase (Fig 3E). Immunoblot analysis confirmed these results. At 9 hours after release from G1/S arrest with aphidicolin, TRAIP expression was already suppressed by RO3306 added 3 hours after release from G1/S arrest. Although RO3306 inhibited cell cycle progression during G2/M phase between 9 h to 15 h after release, the levels of chromatin-bound PCNA were still higher in RO3306-treated cells than in RO3306-untreated cells (Fig3F). These results demonstrated that phosphorylation stabilized TRAIP protein and was required for the robust interaction of TRAIP with PCNA, as well as for the poly-ubiquitinated activity of TRAIP required to dissociate PCNA from chromatin.

TRAIP-mediated removal of PCNA that remains bound to chromatin upon replication stress during mitosis

Mitotic-arrested TRAIP-depleted cells showed retention of PCNA in the chromatin-bound fraction (Fig 1D). Since nocodazole inhibits tubulin polymerization, the cells are arrested at early mitosis. To determine whether PCNA was retained on chromatin during early to late mitosis and not in TRAIP-depleted cells, we performed immunofluorescent detection of PCNA in asynchronous growing cells. As shown Fig 4A, PCNA signals disappeared from chromatin in control cells at early mitosis (prometaphase) and at late mitosis (telophase), indicating that PCNA had dissociated from chromatin by early mitosis through the sequential actions of ATAD5/Elg1-RFC and TRAIP. Conversely, many populations of cells exhibited PCNA signals merging with chromosomes during early to late mitosis in TRAIP-depleted cells.

PCNA was retained on chromatin after entry into mitosis could occur during cell cycle progression. MiDAS (mitotic DNA synthesis) can happen when cells are exposed to replication stress (Minocherhomji et al. 2015). In cells exposed to drugs or containing DNA adducts, DNA synthesis is

slightly delayed and consequently unscheduled DNA synthesis occurs in mitosis in a TRAIP-dependent manner (Sonneville et al. 2019). When cells containing unreplicated DNA enter mitosis, TRAIP mediates the removal of CMG and the DNA is cleaved in a Rad51 dependent manner. This is followed by DNA repair synthesis, which completes the duplication of DNA. The retention of PCNA on mitotic chromatin has already been reported in cells with MiDAS (Minocherhomji et al. 2015; W. Wu et al. 2023). To track chromatin-bound PCNA after the induction of MiDAS, we observed immunofluorescent PCNA signals on chromatin in mitotic cells in asynchronous cultured cells (Fig 4B). When MiDAS was induced by low doses of aphidicolin (0.4mM), the cells not only incorporated EdU but also contained chromatin-bound PCNA during early mitosis. The chromatin-bound PCNA disappeared when cells entered late mitosis. In TRAIP-depleted cells, MiDAS does not occur, because the removal of CMG is impaired. However, chromatin-bound PCNA was detected during early mitosis and even during late mitosis in these cells. These findings demonstrated that chromatin-bound PCNA in cells undergoing MiDAS is completely released via a TRAIP-mediated PCNA removal process.

TRAIP was required for accurate cell cycle progression and correct cell growth

We previously reported that ATAD5/Elg1-depleted cells exhibit S phase delay due to the high level of chromatin-bound PCNA, because ATAD5/Elg1 depletion does not activate the DNA replication checkpoint nor the DNA damage checkpoint response (Shiomi and Nishitani 2013) (Fig 5A and B). Thus, we decided to examine cell cycle progression in TRAIP-depleted cells (Fig 5A). When we monitored the cell cycle profile of asynchronously growing TRAIP-depleted cells, we observed an increase in the population of cells with 4N DNA content, indicating that TRAIP depletion leads to a delay in mitotic progression, in contrast to ATAD5/Elg1-depleted cells. Additionally, depletion of ATAD5/Elg1 in TRAIP-depleted cells synergistically increased the number of cells in both S phase and mitotic cells.

A colony formation assay and measurement of the survival rate also showed that TRAIP is critical for correct cell growth (Fig 5C). Colonies formation and the cell growth of TRAIP-depleted cells was almost half that of control cells. Interestingly, ATAD5/Elg1 and TRAIP double depleted cells exhibited almost the same growth and survival rate as TRAIP only depleted cells, indicating that TRAIP is more crucial for cell cycle progression than ATAD5/Elg1-RFC. The cell growth defect in TRAIP-depleted cells was not due to activation of DNA replication, the DNA damage checkpoint, or the spindle assembly checkpoint (SAC), because activation of Chk1 and gH2AX and chromatin-bound Mad2 were not detected in TRAIP-depleted cells (Fig 5B). Consistent with this result, functional inactivation of TRAIP has been reported to reduced Mad2 recruitment to kinetochores (Chapard et al. 2014). These findings suggest that increased levels of chromatin-bound PCNA in TRAIP-depleted cells, not checkpoint activation, led to a delay in mitotic progression. Together, these results demonstrated that TRAIP has a critical role in the dissociation of PCNA from chromatin that is required for accurate mitotic progression and correct cell growth.

Next, we expressed TRAIP tagged with mAID at its C-terminus in cells to analyze further TRAIP functions throughout the cell cycle (Natsume et al. 2016; Yesbolatova et al. 2020). We monitored TRAIP-mAID degradation and the cell cycle profiles of asynchronous growing cells at the indicated times after addition of auxin (5-ph-IAA). As shown in Fig 5D, TRAIP-mAID was almost completely degraded at 2 hours after 5-ph-IAA addition. The cell cycle profiles (Fig 5E) up to 24 hours after 5-ph-IAA addition revealed a gradual increase in the mitotic cell population, which is consistent with the result of the RNAi experiment (Fig 5A). These results confirmed that TRAIP is required for accurate mitotic progression and exit. At 48 hours after 5ph-IAA addition to asynchronous cells, however, the mitotic cell population decreased and the G1 phase cell population increased gradually. After 72 hours, G1 phase cells represented 44% of the cell population, which was almost the same as that of 5-ph-IAA untreated asynchronous cells. It should be noted that at 24 hours after the addition of

5-ph-IAA, the S phase cell population was much lower than that of the 5-ph-IAA untreated asynchronous cells. These data indicate that although TRAIP depletion delays mitotic progression, cells eventually exit mitosis and enter G1 phase, but afterwards find it difficult to enter S phase.

Next, we arrested TRAIP-mAID cells at the G1/S border with aphidicolin and after release, collected cells at the indicated times to monitor cell cycle profiles and the level of chromatin-bound PCNA (Fig EV4). Since TRAIP bound to PCNA during middle to late S phase (Fig 2F), there was a possibility that TRAIP is also required for the dissociation of PCNA from chromatin during S phase. A comparison of 5-ph-IAA treated cells with untreated control cells, showed that both cells reached late S phase almost at the same time after about 10 hours after release (Fig EV4A). The level of chromatin-bound PCNA was almost at the same in the presence and absence of TRAIP (Fig EV4B). These results demonstrated that although TRAIP was bound to chromatin-loaded PCNA during S phase, it did not participate in the dissociation of PCNA from chromatin during S phase.

Clearance of PCNA from chromatin by TRAIP during mitosis was required for licensing of DNA replication

As described above, TRAIP is required for the dissociation of PCNA from chromatin, not during S phase, but before mitotic exit. Based on this result, we hypothesized that the retention of PCNA on chromatin is detrimental for cell cycle progression during the next G1 phase. During the end of mitosis and subsequent G1 phase, the key event enabling cell cycle progression is the formation of a pre-RC by Cdt1, cdc6, and MCM2-7 on the origin of replication. A defect in pre-RC formation would lead to a delay in entry into S phase.

To test this, TRAIP-mAID expressing cells were released from mitotic arrest with nocodazole, in the absence or presence of 5-ph-IAA. About 90% of the 5-ph-IAA treated and untreated cells showed a 4C DNA content, indicating that these cells were arrested at mitosis by nocodazole (Fig 6A). After

release of the arrested cells into the cell cycle, the 5-ph-IAA untreated cells showed a decrease in the mitotic cell population and progressed into G1 phase and then S phase. At 10 hours after release, over 80% of the cells had progressed into S phase. Conversely, 5-ph-IAA treatment reduced the number of mitotic cells gradually, but the progression of the 5-ph-IAA treated cells into G1 phase was very slow. Although some population of cells exited mitosis and progressed into G1 phase, these cells progressed with difficulty into S phase, as shown in Fig5E. We confirmed this result by releasing TRAIP-mAID-expressing cells arrested at G1 phase with palbociclib into cell cycle in the absence or presence of 5-ph-IAA (Fig EV5). About 60% of the 5-ph-IAA treated and untreated cells showed a 2C DNA content, indicating that most of these cells were arrested at G1 phase. After release into cell cycle, the G1 phase population of the 5-ph-IAA untreated cells progressed into S phase, but TRAIP-mAID depleted cells showed a delay in S phase entry. Next, we checked protein levels, which required for DNA replication, in cells released from mitosis (Fig 6B). In nocodazole-arrested mitotic cells, PCNA was not detected on chromatin in the absence of 5-ph-IAA, but some PCNA was detected on chromatin in the presence of 5-ph-IAA. Four hours after release from mitosis, the level of chromatin-bound PCNA drastically increased in cells without 5-ph-IAA treatment, indicating that some populations of these cells had entered S phase. However, in TRAIP-mAID depleted cells treated with 5-ph-IAA, the increase in chromatin-bound PCNA was smaller, indicating that TRAIP depletion impairs S phase entry. Expectedly, the levels of proteins required for pre-RC progression differed between cells treated with 5-ph-IAA and those untreated with 5-ph-IAA. The levels of Cdt1 and chromatin-bound MCM proteins were reduced in TRAIP-mAID depleted cells. These results were confirmed by immunofluorescence microscopy of Cdt1 in asynchronous growing cells (Fig 6C). To compare the expression levels of Cdt1 during G1 phase between control cells and TRAIP-mAID depleted cells, we excluded S phase cells based on EdU incorporation and mitotic cells based on their chromosomal structure, as revealed by hoechst staining. Additionally, among EdU unincorporated cells, we also excluded G2 phase cells

based on their large nucleus size. In G1 phase cells, Cdt1 was detected in about 68% of cells expressing TRAIP. Conversely, in TRAIP-depleted cells after the addition of 5-ph-IAA, Cdt1 signals were reduced during G1 phase to about 30%. These results demonstrated that TRAIP-mediated clearance of PCNA from chromatin during mitosis is required for adequate mitotic progression and exit. Additionally, TRAIP-depleted cells showed a reduced level of Cdt1, indicating that TRAIP is required for appropriate pre-RC formation during G1 phase via its ability to stabilize Cdt1.

Discussion

In this study, we have shown that TRAIP and p97/VCP are required for optimal cell cycle progression and cell growth via their ability to remove PCNA from chromatin during mitosis. Especially, we showed that retention of PCNA on chromatin during mitosis in TRAIP-depleted cells triggered the degradation of Cdt1, an essential factor for replication licensing, leading to impaired pre-RC formation during the next G1 phase and inhibition of DNA replication initiation.

PCNA release from chromatin is known to be performed by ATAD5/Elg1-RFC, an AAA+ ATPase RFC family member clamp unloader, which requires ATP hydrolysis for its activity (Shiomi and Nishitani 2017; Kang et al. 2019). Cells depleted of ATAD5/Elg1 show a delay in the cell cycle due to the high levels of chromatin-bound PCNA in these cells. ATAD5/Elg1 depletion also leads to the formation of aberrant chromatin structures, demonstrating that appropriate removal of PCNA from chromatin is indispensable for genome integrity and cell homeostasis. These functions of ATAD5/Elg1-RFC appear to be limited to S phase, because PCNA is removed from chromatin during mitosis in ATAD5/Elg1 depleted cells, suggesting that some other PCNA removal system(s) exists in eukaryotic cells (Shiomi and Nishitani 2013).

Unexpectedly, the removal of PCNA from chromatin in mitosis is not regulated by RFC complexes, but by the ubiquitination system. The ubiquitin-dependent molecular chaperone p97/VCP has emerged as an essential regulator of UPS-dependent protein turnover in chromatin. p97/VCP, via its intrinsic ATPase activity, segregates poly-ubiquitinated proteins from diverse cellular locations and presents them for proteasomal degradation. Recently, the functions of p97/VCP in several DNA metabolic processes has indicated that it is a constitutive component of various essential chromatin-related processes during the cell cycle–progression (Vaz, Halder and Ramadan 2013). Especially, during DNA replication, p97/VCP is known to remove CMG from chromatin via its ability to recognize poly-ubiquitinated MCM7.

TRAIP is required for CMG disassembly from chromatin after DNA replication terminates in mitosis and from stalled replisomes in mitosis prior to MiDAS and in S phase prior to ICL repair (Wu, Pellman and Walter 2020). During these processes, TRAIP poly-ubiquitinates MCM7, which is then recognized by p97/VCP, resulting in a change in its conformation. Eventually, CMG is released from chromatin. Curiously, the PIP box is required for the recruitment of TRAIP for ICL repair, but it is not required for CMG disassembly during mitosis (Villa et al. 2021).

A previous report suggested that PCNA is the candidate substrate for TRAIP (Hoffmann et al. 2016), and actually, the regulation of the level of chromatin-bound PCNA by TRAIP has already been reported (Feng et al. 2016). This study, however, was restricted in that it only reported TRAIP-mediated release of chromatin-bound PCNA during DNA damage-induced replication stress. Consistent with this report, we also found that TRAIP drives PCNA dissociation from chromatin after MiDAS is induced by replicative stress. Additionally, we also found that TRAIP removed PCNA from chromatin in mitosis during normal cell cycle progression.

It is possible that impaired removal of CMG from chromatin by depletion of TRAIP was responsible for the various cell phenotypes reported in the present study. Both E3 ubiquitin ligases

CRL2-LRR1 and TRAIP can ubiquitinate MCM7. CRL2-LRR1 is regarded as the main CMG remover, while TRAIP is considered to function as a backup in the absence of CRL2-LRR1 (Villa et al. 2021). However, our results clearly demonstrated that TRAIP is indispensable for the removal of PCNA from chromatin during mitosis, because PCNA was retained on mitotic chromatin after TRAIP depletion.

Our results also indicated that PCNA is poly-ubiquitinated at K164 so that it can be removed from chromatin by p97/VCP. Ubiquitination of K164 is important for the response DNA damage and template switching (Hoege et al. 2002; Stelter and Ulrich 2003), and it promotes translesion synthesis in undisturbed cells (Terai et al. 2010). It is known that mono-ubiquitination or K63-linked poly-ubiquitylation of PCNA switches its normal function to its damage response function (Ripley, Gildenberg and Washington 2020). Mitotic disassembly of CMG by TRAIP also involves the formation of K6- and K63-linked longer ubiquitin chains assembled on Mcm7, and overall the ubiquination pattern is different (Priego Moreno et al. 2019). In this manuscript, although the ubiquitin linkage involved in the mitotic disassembly of PCNA is yet to be elucidated, it seems likely that K6 and K63 ubiquitin linkages are also required.

TRAIP expression increased after onset of S phase, and TRAIP bound to PCNA through its PIP box. Mutation or deletion of the PIP box of TRAIP impaired its ability to associate with chromatin-bound PCNA; thus, the PIP box of TRAIP is indispensable for its association with and ubiquitination of PCNA. We found that PCNA did not dissociate from chromatin during mitosis in cells expressing PIP box-deleted TRAIP. However, these cells simultaneously expressed endogenous and PIP box-deleted TRAIP, suggesting that although the PIP box of TRAIP is required for its stable interaction with PCNA, PIP box-deleted TRAIP may possess another motif for temporal interaction with PCNA that is sufficient to inhibit the function of endogenous TRAIP. Further studies are required

to understand how TRAIP recognize PCNA for ubiquitination.

TRAIP travels with the replisome during DNA elongation and ubiquitinates MCM7 after termination of replication (Hoffmann et al. 2016; Dewar et al. 2017). CMG is the candidate of platform for TRAIP as it travels with the replication fork. However, it has been unclear why TRAIP does not trigger ubiquitylation for the unloading of CMG with which it travels. Our findings indicate that PCNA serves as the main platform for TRAIP association with the replication fork and that this is dependent on stable TRAIP binding to PCNA via its PIP box. Indeed, in TRAIP-mAID depleted cells, the level of chromatin-bound PCNA was not different from that in control cells during S phase, demonstrating that TRAIP does not influence the level of chromatin-bound PCNA during progression of the replication fork. Hence, TRAIP binds to PCNA and travels with the replication fork until it is activated by mitotic phosphorylation.

The phosphorylation of various proteins by CDK1 is required for appropriate mitotic progression. Recently, the coordination of DNA replication and mitosis through the ubiquitin system and CDK1 phosphorylation was reported (Galarreta et al. 2021). Our data suggest that TRAIP is phosphorylated during mitosis. The CDK1 inhibitor, RO3306, blocked the interaction between TRAIP and PCNA and destabilized TRAIP protein. These data indicate that TRAIP requires phosphorylation for its stabilization and association with PCNA during late S phase to mitosis. TRAIP also required phosphorylation for its ubiquitination activity. Indeed, Walter's group demonstrated that ubiquitination of MCM7 is required for CDK1 activity (Wu et al. 2019). On the other hand, our data indicated that ATAD5/Elg1 is also phosphorylated during mitosis (Fig EV3). Our and other studies have demonstrated that ATAD5/Elg1-RFC functions during S phase, but this study is the first to show that TRAIP removes PCNA from chromatin during mitosis. Based on these results, CDK1 phosphorylation would appear not only to stabilize and activate TRAIP activity, but also to switch the PCNA removal

function from that of ATAD5/Elg1-RFC to that of TRAIP during entry into mitosis. Since the phosphorylation sites of CDK1 on both ATAD5/Elg1-RFC and TRAIP have not yet been identified, further studies will be required to identify these sites in order to uncover the molecular mechanism of the phosphorylation-depended switch that results in the TRAIP-dependent removal of PCNA from chromatin.

MiDAS is required for TRAIP to remove stalled replisomes before DNA synthesis (Sonneville et al. 2019). DNA replication stress not only causes MiDAS, but also retains PCNA on chromatin (Minocherhomji et al. 2015). Very recently, PCNA mono-ubiquitination by Rad18 was reported to be required for MiDAS (Wu et al. 2023). In TRAIP-depleted cells, we found that MiDAS is not induced and PCNA remains bound to chromatin (Fig4B). PCNA remained bound to early mitotic chromatin in cells in which MiDAS was induced by replication stress, irrespective of the presence or absence of TRAIP, but was removed from chromatin in late mitosis in a TRAIP-dependent manner. Thus, TRAIP has critical roles for the removal of PCNA from chromatin both during the normal cell cycle and during replication stress-induced MiDAS.

At the end of mitosis and subsequent G1 phase, a pre-RC is formed through the association of Cdt1, cdc6, and MCM2-7 with the origin of replication. Cdt1 is the key regulator of DNA replication licensing, because it is rapidly degraded after the onset of DNA replication to avoid re-licensing of DNA replication during S phase. Cdt1 degradation is regulated by two independent E3 ubiquitin ligases, CRL1-Skp2 and CRL4-Cdt2. The functions of CRL4-Cdt2 are controlled by chromatin-loaded PCNA (Nishitani and Lygerou 2004; Havens and Walter 2011). CRL4-Cdt2 recognizes via its PIP degron formed by Cdt1 bound to chromatin-loaded PCNA. Finally, Cdt1 is poly-ubiquitinated and degraded by proteolysis. PCNA does not bind to chromatin during G1 phase of the normal cell cycle,

but when cells suffer DNA damage caused by such as agents as UV irradiation, PCNA is loaded onto chromatin for DNA repair, after which Cdt1 is degraded in a CRL4-Cdt2-dependent manner. Thus, PCNA bound to chromatin in TRAIP-depleted cells seems to trigger Cdt1 degradation.

Previously, we reported that when mitotic cells were irradiated UV, Cdt1 became resistant to degradation. However, when these cells were released and allowed to progress into G1 phase, PCNA was loaded onto chromatin for DNA repair and Cdt1 was degraded by CRL4-Cdt2 in a chromatin-bound PCNA-dependent fashion, and DNA replication licensing was severely inhibited. Such cells had a high frequency of cell cycle arrest during G1 phase. Thus, our data suggested that in addition to the well-known DNA damage checkpoint response, cells have a replication licensing checkpoint that links mitotic DNA damage to cell cycle control (Morino et al. 2015). We also found that TRAIP is required for the dissociation of PCNA from chromatin, and that impairment of this mechanism leads to the retention of PCNA on chromatin during mitosis to G1 phase. Hence, TRAIP seems to play critical roles as the guardian of the licensing checkpoint. Although further experiments will be required to further understand the relationships between TRAIP function and DNA replication licensing, our findings provide new insights into replication licensing.

As described as above, defects in the removal of PCNA from chromatin by ATAD5/Elg1-RFC and TRAIP can jeopardize genome integrity. The depletion of ATAD5/Elg1 delays S phase progression, results in aberrant regulation of chromosomal proteins, and leads to chromosomal abnormalities. Depletion of TRAIP results in defects in mitotic progression, mitotic exit, and pre-RC formation during G1 phase. These differences in the functions of ATAD5/Elg1-RFC and TRAIP can be attributed to differences in the timing of their functions or differences in the states of PCNA. Although PCNA travels with the replisome while changing binding partners and is modified during replication fork progression, PCNA is liberated at the termination of replication. It is possible that the

differences in the molecular states of PCNA limit the ubiquitination by TRAIP or unloading by ATAD5/Elg1.

Our results also demonstrated that not only TRAIP, but also ATAD5/Elg1 were reduced during G1 phase, these data indicating that the functions of PCNA dissociation from chromatin are declined in G1 phase. In TRAIP-depleted cells, however, cells progressed into the cell cycle and entered S phase despite impaired pre-RC formation. These results suggested that the dissociation of PCNA from chromatin in G1 phase occurs via an unknown mechanism. Of course, the relatively short half-life of chromatin-bound PCNA could result in PCNA dissociation from chromatin in G1 phase even in TRAIP defective cells (Sasaki et al. 1995). Further studies will be required to understand how PCNA is removed from chromatin to ensure faithful genome integrity.

DNA replication occurs once per cell cycle before cell division to maintain genome integrity. DNA replication can be divided into three stages, initiation, elongation, and termination. One key event during initiation is the assembly of CMG at origins of replication (Costa and Diffley 2022). Once DNA replication is initiated, PCNA is loaded onto DNA at every primed sites during elongation and orchestrates the activities of functional proteins required replication, repair, recombination, and chromosomal architectures. PCNA is unloaded from chromatin at sites of DNA ligation and nucleosome re-assembly (Waga and Stillman 1998; Burgers and Kunkel 2017). Recently, studies on DNA replication have focused on the molecular mechanisms of disassembly of the replisome during replication termination (Gambus 2017; Dewar and Walter 2017). In this study, we report a novel pathway for the removal of PCNA from chromatin during replication termination. We also report that the mechanism during replication termination that is required for precise replication initiation. Thus, the release of chromatin-bound PCNA by TRAIP is critical for linking replication termination to the next initiation to maintain genome stability, integrity, and homeostasis during cell cycle progression

and faithful cell growth.

Material and Methods

Construction of GFP-TRAIP expressed plasmids

Total mRNA was collected from U2OS cells with NucleoSpin RNA XS (740902.50; Macherey-Nagel). To construct N-terminally GFP-tagged TRAIP (WT, mPIP or ΔPIP), the following primer sets were used for RT-PCR to amplified TRAIP cDNA, and the fragment was inserted into KpnI and BamHI sites of the pAcGFP1-Hyg-C1 plasmid. The primer sets were: (F) ATATAGGTACCATGCCTATCCGTGCTCTGTGC and (R) ATATATGGATCCTCACGACCACAGGAAGGTGTCCAGC for WT, (R) ATATATGGATCCTCACGACCACAGGGCGGTGTCCAGC for mPIP or (R) ATATATGGATCCTCAGAAGAGAGAAGGCACTGTC for DPIP.

Each cell line stably expressing GFP-TRAIP was established by transfecting each pGFP-TRAIP (WT, mPIP or ΔPIP) plasmid into U2OS cells and screening for Hygromycin B resistance

Establishment of HCT116 cell lines expressing mAID-ATAD5/Elg1 and TRAIP-mAID

A CRISPR-Cas9 plasmid targeting the region adjacent to the start codon of the ATAD5/Elg1 gene (CACCGGCTGTGGTACCAGGTCACG/agg) was constructed using pX330-U6-Chimeric_BB-CBh-hSpCas9 (Addgene 42230) (Ran et al. 2013). A donor plasmid containing the Hygro-P2A-mAID tag was constructed according to the published protocol (Natsume et al. 2016). Parental HCT116 cells conditionally expressing Tet-OsTIR1 were transfected with CRISPR-Cas9 and donor plasmids followed by selection in the presence of 100 μg/mL Hygromycin B (#ant-hg-1; InvivoGen). To establish the TRAIP-mAID cell line, a CRISPR-Cas9 plasmid targeting the region

adjacent to the stop codon of the TRAIP gene (CTCACTGTTCTCACGACCAC/agg) using pX330 and a donor plasmid containing the mAID-Clover (mAC) tag were constructed. These plasmids were transfected into HCT116 cells expressing OsTIR1 (F74G) followed by selection in the presence of Hygromycin B (Saito and Kanemaki, 2021; Yesbolatova et al., 2020, 2019). After colony isolation, clones harboring bi-allelic insertion at the target locus were verified by genomic PCR. The expression and degradation of target proteins were confirmed by immunoblotting.

Cell culture

Hela and U2OS cell lines were cultured in Dulbecco's modified Eagle's medium (DMEM)(11995-065; Gibco) with 10 % fetal bovine serum and 1 % Penicillin-Streptomycin Solution (P4333; Sigma-Aldrich) at 37℃ in a 5 % CO_2 atmosphere. The cell lines stably expressing GFP-TRAIP were cultured in DMEM with Hygromycin B (ant-hg-1; InvivoGen). HCT116 cell lines were cultured in McCoy's 5A medium (McCoy's)(16600-082; Gibco) instead of DMEM as described above. The HCT116 cells expressing OsTIR1 and mAID-ATAD5/Elg1 or TRAIP-mAID were cultured in McCoy's with HygromycinB.

To deplete p97/VCP, TRAIP, LRR1, and ATAD5/Elg1 by RNAi, siRNAs (HSS111263 for p97/VCP, HSS129125 for TRAIP, HSS151229 for LRR1 and HSS129125 for ATAD5/Elg1, from Invitrogen) were transfected at 100 μM using HiPerFect (Qiagen). Twenty-four hours after the first transfection, the second transfection was carried out, and the cells were cultured for two more days.

To arrest the cells at G1 phase and mitosis, cells were treated with 20 μM Lovastatin or 1μM Palbocicrib for 48 h, and 0.1 μg/ml nocodazole for 24 h, respectively. To synchronize cells in early S phase, cells were treated with 2 mM thymidine or 5μg/ml aphidicolin for 24 h. The synchronized cells were released into the cell cycle by washing them sequentially three times each with PBS and medium. The cells were then collected at the indicated times. To inhibit CDK1, cells

were released 1 or 3 h after synchronization in early S phase and then cultured in medium containing 10 μM RO3306 for the indicated times. To deplete mAID-ATAD5/Elg1 or TRAIP-mAID, cells were cultured in McCoy's medium with 2 μg/ml doxycycline and 500μM IAA or 1μM 5-Ph-IAA, respectively. T2AA and RO3306 were purchased from Cayman chemical and Calbiochem, respectively.

To induce MiDAS, 0.4μM aphidicolin was added to asynchronously growing cells for 24 h, and after release, the cells were treated with 10μM of EdU for 15min and EdU incorporation was detected using Click-IT chemistry following the manufacturer's instructions (Click-IT EdU; Alexa fluor 488, Imaging Kits, Life Technologies).

To analyze cell cycle profiles according to DNA content, flow cytometry was performed with FACSMelody and FACSChorus software, and the cell populations with various DNA contents were analyzed with ModFit LT software (Becton Dickinson).

Immunoblotting

For immunoblotting, cultured cells were treated with 0.5 % trypsin and centrifuged (700 g for 5 min at 4 °C). Cells were then washed with PBS and lysed in mCSK buffer (100 mM NaCl, 10 mM Pipes (pH 7.0), 300 mM sucrose, 0.1 % Triton X-100, 1 mM $MgCl_2$, 1 mM EDTA) containing 1×Protease inhibitor cocktail (11697498001; Roche Diagnostics) for 10 min on ice. Protein concentration was determined by the Bradford assay, and whole cell extracts were subjected to SDS-PAGE electrophoresis after diluting them at a ratio of 1:1 in Laemmli buffer (25 mM Tris-HCl (pH 6.8), 50 mM dithiothreitol, 1 % SDS, 5 % glycerol, 0.05 % bromophenol blue) followed by boiling for 10 min at 95°C. To prepare the chromatin fraction, after centrifugation of half of the cell extracts (11,400 g for 1 min at 4°C), precipitates were washed with the same volume of mCSK buffer and then suspended in same volume of Laemmli buffer and boiled. Total amounts of protein were adjusted to

load 2.5 μg of whole cell extract and 5 μg or 10 μg of chromatin fraction onto SDS-polyacrylamide gels. The following antibodies were used as primary antibodies: TRAIP (AG0491; Proteintech), PCNA (sc-56; Santa Cruz), phospho-histone H3 (Ser10)(06-570; Sigma-Aldrich), H3 (AG10644; Proteintech), MCM5 (11703-1-AP; Ptoteintech), MCM6 (13347-2-AP; Ptoteintech), Chk1 (2345; Cell Signaling), phospho-Chk1 (Ser 296) (2349; Cell Signaling), H2A (3636; Cell Signaling), γH2AX (05-636; Millipore), and p97/VCP (2648; Cell Signaling). ATAD5/Elg1 antibodies were raised in rabbits against a synthetic peptide containing aa 183 to aa 210 of human ATAD5. Antibodies for Cdt1 and MCM2 have been described previously (Nishitani et al. 2001; Nishitani et al. 2014). The following antibodies were used as secondary antibodies: anti-mouse IgG (NA0310V; GE Healthcare) and anti-rabbit IgG (NA9340V; GE Healthcare). Protein levels were calculated by examining band densities with ImageJ software.

Fluorescent microscopy

For fluorescent microscopy, the cells were fixed in 4 % paraformaldehyde for 5 min, washed three times with PBS, and then permeabilized in 0.1 % TritonX-100 in PBS for 1 min. For pre-extract treatment, cells were permeabilized in ice cold PBS containing 0.1 % TritonX-100 for 5 min, before fixation as described above. To measure PCNA immunofluorescence, cells were permeabilized in -30°C methanol for 5 min instead of in TritonX-100. Cells were treated with blocking buffer (3 % bovine serum albumin and 0.2 % Tween 20, 0.005 % NaN_3) at room temperature for 1 h, washed three times with PBS, and stained with the following primary antibodies: Cdt1 (Nishitani et al. 2001), Cyclin A (Ab-6; Thermo Fisher Scientific), Cyclin B (sc-245; Santa Cruz), or PCNA (sc-56; Santa Cruz). After washing the cells three times with PBS, the cells were stained with the following secondary antibodies: Red anti-mouse antibody (A11032; Molecular Probes) or Red anti-rabbit antibody (A11037; Molecular Probes). To visualize DNA, hoechst 33258 was used.

To identify S phase cells, cells treated with 10μM of EdU for 10min and incorporated EdU was detected using Click-IT chemistry.

Acknowledgments

We thank Inoue and Kusaka (Univ. of Hyogo) for initial experiment of this work. We also thank Natsume (NIG), Shimizu and Matsubara (Univ. of Hyogo) for experimental support. This work was supported by JSPS KAKENHI (JP16K07257) to YaS, JSPS KAKENHI (JP21H0419 and JP22H04703) and JST CREST (JPMJCR21E6) to MTK, JSPS KAKENHI (JP20K06547) to HN.

Author Contributions

YaS performed the experiments described in Figures 1, 4, 5, 6A and 6B, and Expanded View Figures EV1, EV2, EV3 and EV5. AT performed the experiments described in Figures 2, 3 and 6C, and Expanded View Figures EV4. YuS and MTK performed AID strain construction. YaS conceived the study, designed the experiments and wrote the manuscript. HN supervising the work.

Conflict of interest

We declare that we have no conflict of interest.

References

Burger, J., Merlet, J., Tavernier, N., Richaudeau, B., Arnold, A., Ciosk, R., Bowerman, B., Pintard, L., 2013. CRL2(LRR-1) E3-ligase regulates proliferation and progression through meiosis in the Caenorhabditis elegans germline. PLoS Genet. 9, e1003375. https://doi.org/10.1371/journal.pgen.1003375

Burgers, P.M.J., Kunkel, T.A., 2017. Eukaryotic DNA Replication Fork. Annu. Rev. Biochem. 86,

417–438. https://doi.org/10.1146/annurev-biochem-061516-044709

Celis, J.E., Celis, A., 1985. Cell cycle-dependent variations in the distribution of the nuclear protein cyclin proliferating cell nuclear antigen in cultured cells: subdivision of S phase. Proc. Natl. Acad. Sci. U. S. A. 82, 3262–3266. https://doi.org/10.1073/pnas.82.10.3262

Chagin, V.O., Casas-Delucchi, C.S., Reinhart, M., Schermelleh, L., Markaki, Y., Maiser, A., Bolius, J.J., Bensimon, A., Fillies, M., Domaing, P., Rozanov, Y.M., Leonhardt, H., Cardoso, M.C., 2016. 4D Visualization of replication foci in mammalian cells corresponding to individual replicons. Nat. Commun. 7, 11231. https://doi.org/10.1038/ncomms11231

Chapard, C., Hohl, D., Huber, M., 2015. The TRAF-interacting protein (TRAIP) is a novel E2F target with peak expression in mitosis. Oncotarget 6, 20933–20945. https://doi.org/10.18632/oncotarget.3055

Chapard, C., Meraldi, P., Gleich, T., Bachmann, D., Hohl, D., Huber, M., 2014. TRAIP is a regulator of the spindle assembly checkpoint. J. Cell Sci. 127, 5149–5156. https://doi.org/10.1242/jcs.152579

Costa, A., Diffley, J.F.X., 2022. The Initiation of Eukaryotic DNA Replication. Annu. Rev. Biochem. 91, 107–131. https://doi.org/10.1146/annurev-biochem-072321-110228

Deegan, T.D., Mukherjee, P.P., Fujisawa, R., Polo Rivera, C., Labib, K., 2020. CMG helicase disassembly is controlled by replication fork DNA, replisome components and a ubiquitin threshold. eLife 9, e60371. https://doi.org/10.7554/eLife.60371

Deng, L., Wu, R.A., Sonneville, R., Kochenova, O.V., Labib, K., Pellman, D., Walter, J.C., 2019. Mitotic CDK Promotes Replisome Disassembly, Fork Breakage, and Complex DNA Rearrangements. Mol. Cell 73, 915-929.e6. https://doi.org/10.1016/j.molcel.2018.12.021

Dewar, J.M., Low, E., Mann, M., Räschle, M., Walter, J.C., 2017. CRL2Lrr1 promotes unloading of the vertebrate replisome from chromatin during replication termination. Genes Dev. 31, 275–290. https://doi.org/10.1101/gad.291799.116

Dewar, J.M., Walter, J.C., 2017. Mechanisms of DNA replication termination. Nat. Rev. Mol. Cell Biol. 18, 507–516. https://doi.org/10.1038/nrm.2017.42

Feng, W., Guo, Y., Huang, J., Deng, Y., Zang, J., Huen, M.S.-Y., 2016. TRAIP regulates replication fork recovery and progression via PCNA. Cell Discov. 2, 16016. https://doi.org/10.1038/celldisc.2016.16

Galarreta, A., Valledor, P., Fernandez-Capetillo, O., Lecona, E., 2021. Coordinating DNA Replication and Mitosis through Ubiquitin/SUMO and CDK1. Int. J. Mol. Sci. 22, 8796. https://doi.org/10.3390/ijms22168796

Gambus, A., 2017. Termination of Eukaryotic Replication Forks. Adv. Exp. Med. Biol. 1042, 163–187. https://doi.org/10.1007/978-981-10-6955-0_8

Han, Y.G., Yun, M., Choi, M., Lee, S.-G., Kim, H., 2019. TRAIP regulates Histone H2B

monoubiquitination in DNA damage response pathways. Oncol. Rep. 41, 3305–3312. https://doi.org/10.3892/or.2019.7092

Harley, M.E., Murina, O., Leitch, A., Higgs, M.R., Bicknell, L.S., Yigit, G., Blackford, A.N., Zlatanou, A., Mackenzie, K.J., Reddy, K., Halachev, M., McGlasson, S., Reijns, M.A.M., Fluteau, A., Martin, C.-A., Sabbioneda, S., Elcioglu, N.H., Altmüller, J., Thiele, H., Greenhalgh, L., Chessa, L., Maghnie, M., Salim, M., Bober, M.B., Nürnberg, P., Jackson, S.P., Hurles, M.E., Wollnik, B., Stewart, G.S., Jackson, A.P., 2016. TRAIP promotes DNA damage response during genome replication and is mutated in primordial dwarfism. Nat. Genet. 48, 36–43. https://doi.org/10.1038/ng.3451

Havens, C.G., Walter, J.C., 2011. Mechanism of CRL4(Cdt2), a PCNA-dependent E3 ubiquitin ligase. Genes Dev. 25, 1568–1582. https://doi.org/10.1101/gad.2068611

Hoege, C., Pfander, B., Moldovan, G.-L., Pyrowolakis, G., Jentsch, S., 2002. RAD6-dependent DNA repair is linked to modification of PCNA by ubiquitin and SUMO. Nature 419, 135–141. https://doi.org/10.1038/nature00991

Hoffmann, S., Smedegaard, S., Nakamura, K., Mortuza, G.B., Räschle, M., Ibañez de Opakua, A., Oka, Y., Feng, Y., Blanco, F.J., Mann, M., Montoya, G., Groth, A., Bekker-Jensen, S., Mailand, N., 2016. TRAIP is a PCNA-binding ubiquitin ligase that protects genome stability after replication stress. J. Cell Biol. 212, 63–75. https://doi.org/10.1083/jcb.201506071

Kang, M.-S., Ryu, E., Lee, S.-W., Park, J., Ha, N.Y., Ra, J.S., Kim, Y.J., Kim, J., Abdel-Rahman, M., Park, S.H., Lee, K.-Y., Kim, H., Kang, S., Myung, K., 2019. Regulation of PCNA cycling on replicating DNA by RFC and RFC-like complexes. Nat. Commun. 10, 2420. https://doi.org/10.1038/s41467-019-10376-w

Kelch, B.A., Makino, D.L., O'Donnell, M., Kuriyan, J., 2012. Clamp loader ATPases and the evolution of DNA replication machinery. BMC Biol. 10, 34. https://doi.org/10.1186/1741-7007-10-34

Kubota, T., Nishimura, K., Kanemaki, M.T., Donaldson, A.D., 2013. The Elg1 replication factor C-like complex functions in PCNA unloading during DNA replication. Mol. Cell 50, 273–280. https://doi.org/10.1016/j.molcel.2013.02.012

Lee, K., Fu, H., Aladjem, M.I., Myung, K., 2013. ATAD5 regulates the lifespan of DNA replication factories by modulating PCNA level on the chromatin. J. Cell Biol. 200, 31–44. https://doi.org/10.1083/jcb.201206084

Li, N., Wang, J., Wallace, S.S., Chen, J., Zhou, J., D'Andrea, A.D., 2020. Cooperation of the NEIL3 and Fanconi anemia/BRCA pathways in interstrand crosslink repair. Nucleic Acids Res. 48, 3014–3028. https://doi.org/10.1093/nar/gkaa038

Maric, M., Maculins, T., De Piccoli, G., Labib, K., 2014. Cdc48 and a ubiquitin ligase drive disassembly of the CMG helicase at the end of DNA replication. Science 346, 1253596. https://doi.org/10.1126/science.1253596

Maric, M., Mukherjee, P., Tatham, M.H., Hay, R., Labib, K., 2017. Ufd1-Npl4 Recruit Cdc48 for Disassembly of Ubiquitylated CMG Helicase at the End of Chromosome Replication. Cell Rep. 18, 3033–3042. https://doi.org/10.1016/j.celrep.2017.03.020

Masai, H., Matsumoto, S., You, Z., Yoshizawa-Sugata, N., Oda, M., 2010. Eukaryotic chromosome DNA replication: where, when, and how? Annu. Rev. Biochem. 79, 89–130. https://doi.org/10.1146/annurev.biochem.052308.103205

Merlet, J., Burger, J., Tavernier, N., Richaudeau, B., Gomes, J.-E., Pintard, L., 2010. The CRL2LRR-1 ubiquitin ligase regulates cell cycle progression during C. elegans development. Dev. Camb. Engl. 137, 3857–3866. https://doi.org/10.1242/dev.054866

Minocherhomji, S., Ying, S., Bjerregaard, V.A., Bursomanno, S., Aleliunaite, A., Wu, W., Mankouri, H.W., Shen, H., Liu, Y., Hickson, I.D., 2015. Replication stress activates DNA repair synthesis in mitosis. Nature 528, 286–290. https://doi.org/10.1038/nature16139

Moreno, S.P., Bailey, R., Campion, N., Herron, S., Gambus, A., 2014. Polyubiquitylation drives replisome disassembly at the termination of DNA replication. Science 346, 477–481. https://doi.org/10.1126/science.1253585

Morino, M., Nukina, K., Sakaguchi, H., Maeda, T., Takahara, M., Shiomi, Y., Nishitani, H., 2015. Mitotic UV irradiation induces a DNA replication-licensing defect that potentiates G1 arrest response. PloS One 10, e0120553. https://doi.org/10.1371/journal.pone.0120553

Mukherjee, P.P., Labib, K.P.M., 2019. In Vitro Reconstitution Defines the Minimal Requirements for Cdc48-Dependent Disassembly of the CMG Helicase in Budding Yeast. Cell Rep. 28, 2777-2783.e4. https://doi.org/10.1016/j.celrep.2019.08.026

Natsume, T., Kiyomitsu, T., Saga, Y., Kanemaki, M.T., 2016. Rapid Protein Depletion in Human Cells by Auxin-Inducible Degron Tagging with Short Homology Donors. Cell Rep. 15, 210–218. https://doi.org/10.1016/j.celrep.2016.03.001

Nishitani, H., Lygerou, Z., 2004. DNA replication licensing. Front. Biosci. J. Virtual Libr. 9, 2115–2132. https://doi.org/10.2741/1315

Nishitani, H., Morino, M., Murakami, Y., Maeda, T., Shiomi, Y., 2014. Chromatin fractionation analysis of licensing factors in mammalian cells. Methods Mol. Biol. Clifton NJ 1170, 517–527. https://doi.org/10.1007/978-1-4939-0888-2_28

Nishitani, H., Taraviras, S., Lygerou, Z., Nishimoto, T., 2001. The human licensing factor for DNA replication Cdt1 accumulates in G1 and is destabilized after initiation of S-phase. J. Biol. Chem. 276, 44905–44911. https://doi.org/10.1074/jbc.M105406200

Ohashi, E., Tsurimoto, T., 2017. Functions of Multiple Clamp and Clamp-Loader Complexes in Eukaryotic DNA Replication, in: Masai, H., Foiani, M. (Eds.), DNA Replication, Advances in Experimental Medicine and Biology. Springer Singapore, Singapore, pp. 135–162. https://doi.org/10.1007/978-981-10-6955-0_7

Papouli, E., Chen, S., Davies, A.A., Huttner, D., Krejci, L., Sung, P., Ulrich, H.D., 2005. Crosstalk between SUMO and ubiquitin on PCNA is mediated by recruitment of the helicase Srs2p. Mol. Cell 19, 123–133. https://doi.org/10.1016/j.molcel.2005.06.001

Pfander, B., Moldovan, G.-L., Sacher, M., Hoege, C., Jentsch, S., 2005. SUMO-modified PCNA recruits Srs2 to prevent recombination during S phase. Nature 436, 428–433. https://doi.org/10.1038/nature03665

Priego Moreno, S., Jones, R.M., Poovathumkadavil, D., Scaramuzza, S., Gambus, A., 2019. Mitotic replisome disassembly depends on TRAIP ubiquitin ligase activity. Life Sci. Alliance 2. https://doi.org/10.26508/lsa.201900390

Punchihewa, C., Inoue, A., Hishiki, A., Fujikawa, Y., Connelly, M., Evison, B., Shao, Y., Heath, R., Kuraoka, I., Rodrigues, P., Hashimoto, H., Kawanishi, M., Sato, M., Yagi, T., Fujii, N., 2012. Identification of small molecule proliferating cell nuclear antigen (PCNA) inhibitor that disrupts interactions with PIP-box proteins and inhibits DNA replication. J. Biol. Chem. 287, 14289–14300. https://doi.org/10.1074/jbc.M112.353201

Ran, F.A., Hsu, P.D., Wright, J., Agarwala, V., Scott, D.A., Zhang, F., 2013. Genome engineering using the CRISPR-Cas9 system. Nat. Protoc. 8, 2281–2308. https://doi.org/10.1038/nprot.2013.143

Ripley, B.M., Gildenberg, M.S., Washington, M.T., 2020. Control of DNA Damage Bypass by Ubiquitylation of PCNA. Genes 11. https://doi.org/10.3390/genes11020138

Saito, Y., Kanemaki, M.T., 2021. Targeted Protein Depletion Using the Auxin-Inducible Degron 2 (AID2) System. Curr. Protoc. 1, e219. https://doi.org/10.1002/cpz1.219

Sasaki, K., Kurose, A., Uesugi, N., Kato, A., 1995. Effects of cycloheximide on chromatin-bound and -unbound PCNA in HeLa cells. Oncology 52, 419–421. https://doi.org/10.1159/000227500

Shiomi, Y., Nishitani, H., 2017. Control of Genome Integrity by RFC Complexes; Conductors of PCNA Loading onto and Unloading from Chromatin during DNA Replication. Genes 8, E52. https://doi.org/10.3390/genes8020052

Shiomi, Y., Nishitani, H., 2013. Alternative replication factor C protein, Elg1, maintains chromosome stability by regulating PCNA levels on chromatin. Genes Cells 18, 946–959. https://doi.org/10.1111/gtc.12087

Sonneville, R., Bhowmick, R., Hoffmann, S., Mailand, N., Hickson, I.D., Labib, K., 2019. TRAIP drives replisome disassembly and mitotic DNA repair synthesis at sites of incomplete DNA replication. eLife 8. https://doi.org/10.7554/eLife.48686

Sonneville, R., Moreno, S.P., Knebel, A., Johnson, C., Hastie, C.J., Gartner, A., Gambus, A., Labib, K., 2017. CUL-2LRR-1 and UBXN-3 drive replisome disassembly during DNA replication termination and mitosis. Nat. Cell Biol. 19, 468–479. https://doi.org/10.1038/ncb3500

Soo Lee, N., Jin Chung, H., Kim, H.-J., Yun Lee, S., Ji, J.-H., Seo, Y., Hun Han, S., Choi, M., Yun, M., Lee, S.-G., Myung, K., Kim, Y., Chul Kang, H., Kim, H., 2016. TRAIP/RNF206 is required

for recruitment of RAP80 to sites of DNA damage. Nat. Commun. 7, 10463. https://doi.org/10.1038/ncomms10463

Stelter, P., Ulrich, H.D., 2003. Control of spontaneous and damage-induced mutagenesis by SUMO and ubiquitin conjugation. Nature 425, 188–191. https://doi.org/10.1038/nature01965

Terai, K., Abbas, T., Jazaeri, A.A., Dutta, A., 2010. CRL4(Cdt2) E3 ubiquitin ligase monoubiquitinates PCNA to promote translesion DNA synthesis. Mol. Cell 37, 143–149. https://doi.org/10.1016/j.molcel.2009.12.018

Vaz, B., Halder, S., Ramadan, K., 2013. Role of p97/VCP (Cdc48) in genome stability. Front. Genet. 4, 60. https://doi.org/10.3389/fgene.2013.00060

Villa, F., Fujisawa, R., Ainsworth, J., Nishimura, K., Lie-A-Ling, M., Lacaud, G., Labib, K.P., 2021. CUL2LRR1 , TRAIP and p97 control CMG helicase disassembly in the mammalian cell cycle. EMBO Rep. e52164. https://doi.org/10.15252/embr.202052164

Waga, S., Stillman, B., 1998. The DNA replication fork in eukaryotic cells. Annu. Rev. Biochem. 67, 721–751. https://doi.org/10.1146/annurev.biochem.67.1.721

Wallace, H.A., Merkle, J.A., Yu, M.C., Berg, T.G., Lee, E., Bosco, G., Lee, L.A., 2014. TRIP/NOPO E3 ubiquitin ligase promotes ubiquitylation of DNA polymerase η. Dev. Camb. Engl. 141, 1332–1341. https://doi.org/10.1242/dev.101196

Wu, R.A., Pellman, D.S., Walter, J.C., 2020. The Ubiquitin Ligase TRAIP: Double-Edged Sword at the Replisome. Trends Cell Biol. https://doi.org/10.1016/j.tcb.2020.11.007

Wu, W., Barwacz, S.A., Bhowmick, R., Lundgaard, K., Gonçalves Dinis, M.M., Clausen, M., Kanemaki, M.T., Liu, Y., 2023. Mitotic DNA synthesis in response to replication stress requires the sequential action of DNA polymerases zeta and delta in human cells. Nat. Commun. 14, 706. https://doi.org/10.1038/s41467-023-35992-5

Yesbolatova, A., Natsume, T., Hayashi, K.-I., Kanemaki, M.T., 2019. Generation of conditional auxin-inducible degron (AID) cells and tight control of degron-fused proteins using the degradation inhibitor auxinole. Methods San Diego Calif 164–165, 73–80. https://doi.org/10.1016/j.ymeth.2019.04.010

Yesbolatova, A., Saito, Y., Kitamoto, N., Makino-Itou, H., Ajima, R., Nakano, R., Nakaoka, H., Fukui, K., Gamo, K., Tominari, Y., Takeuchi, H., Saga, Y., Hayashi, K.-I., Kanemaki, M.T., 2020. The auxin-inducible degron 2 technology provides sharp degradation control in yeast, mammalian cells, and mice. Nat. Commun. 11, 5701. https://doi.org/10.1038/s41467-020-19532-z

Figure legends

Figure 1. PCNA was removed from chromatin by TRAIP and p97/VCP

(A) Asynchronous (phase; A) and mitosis-arrested (phase; M) HCT116 cells expressing mAID-ATAD5/Elg1 were lysed and separated into whole cell extract (WCE) fractions and chromatin fractions (Chr), and the fractions were immunoblotted using the indicated antibodies. Before collecting cells, auxin (IAA) or T2AA was added to deplete the mAID-ATAD5/Elg1 and inhibit the interaction between PCNA and PIP-containing proteins, respectively. The levels of chromatin-bound PCNA (normalized to PCNA in WCE) were quantified and are indicated under the immunoblot bands relative to those of untreated asynchronous cells set as 1.0.

(B) Asynchronous (A) and mitosis-arrested (M) HCT116 cells with and without ~~depletion of~~ p97/VCP depletion were lysed and separated into WCE and Chr fractions, and the fractions were immunoblotted with the indicated antibodies.

(C) Long exposure of the immunoblot shown in (B).

(D) Asynchronous (A) and mitosis-arrested (M) HCT116 cells with and without TRAIP depletion were lysed and separated into WCE and Chr fractions, and the fractions were immunoblotted with the indicated antibodies. The asterisk indicates a non-specific band.

(E) Asynchronous (A) and mitosis-arrested (M) U2OS cells transiently expressing 6myc tagged WT or K164R mutated PCNA were lysed and separated into WCE and Chr fractions, and the indicated proteins were detected using specific antibodies.

Figure 2. TRAIP expression increased after the onset of S phase and TRAIP interacted with PCNA through its PIP box

(A) U2OS cells arrested at G1/S phase with a thymidine block (Thy) were released into S phase and collected at the indicated times. Cells were also arrested at mitosis and G1 phase by adding nocodazole (Noco) and lovastatin (Lova), respectively. The WCE and Chr fractions were immunoblotted with the

indicated antibodies. The levels of chromatin-bound PCNA (normalized to the PCNA level in WCE) are indicated by solid dots and lines, relative to those in asynchronous cells set as 1.0. The levels of TRAIP are indicated by vertical bars and dashed lines with errors, relative to those in asynchronous cells set as 1.0. A graph of the levels of TRAIP obtained from five independent experiments is shown.

(B) Schematic structure of human TRAIP tagged with GFP at its N-terminus. The mutated site of TRAIP (mPIP and ΔPIP) is indicated on the left.

(C) Expression of GFP-TRAIP in U2OS cells growing asynchronously (A) or arrested at mitosis (M). GFP-tagged and endogenous TRAIP were detected using an anti-TRAIP antibody. The positions of GFP-tagged and endogenous TRAIP are indicated by arrows.

(D) Cdt1, Cyclin A, and Cyclin B immunofluorescence (cyan) in asynchronously growing GFP-TRAIP (green) expressing cells. The percentages of overlap between green and cyan signals are indicated at the right in merged pictures. The bar indicates 20 μm.

(E) U2OS cells expressing GFP-TRAIP (green) were arrested at G1/S phase with a thymidine block (0h) and after release into S phase, the cells were collected at the indicated times. The percentages of overlap between the green and blue (DNA) signals are indicated at the bottom of the images. The bar indicates 20 μm.

(F) Endogenous PCNA immunofluorescence (cyan) in pre-extract treated asynchronously growing U2OS cells expressing GFP-TRAIP (green). S phase was divided into early, mid, and late phases according to the PCNA foci pattern. The cells that did not exhibit PCNA foci were considered G1 phase cells. The bar indicates 10 μm.

Figure 3. PIP box and phosphorylation of TRAIP are required for TRAIP association with PCNA and removal of PCNA from chromatin

(A) Asynchronous (Asy) of GFP-TRAIP (WT, mPIP and ΔPIP) expressing cells and 9 hours after

their release from the G1/S arrest with a thymidine block (Late S). The percentages of overlap between green (GFP-TRAIP) and blue (DNA) signals are indicated at the bottom of the images. The bar indicates 20 μm.

(B) GFP-TRAIP (WT, mPIP and ΔPIP) expressing cells arrested at G1/S phase with a thymidine block and released for 9 hours to late S phase. GFP-TRAIP (green) fluorescence was observed with endogenous PCNA detected by immunofluorescence (cyan) after pre-extract treatment. The percentages of overlap between green and cyan signals are indicated at the right of the merged images. The bar indicates 5 μm.

(C) WCE and Chr fractions of asynchronous (A) and mitosis-arrested (M) U2OS cells and GFP-TRAIP (WT, ΔPIP) expressing cells were immunoblotted with the indicated antibodies. The levels of chromatin-bound MCM5 and PCNA (normalized to the level of each protein in the WCE) are indicated by vertical bars with errors, relative to those in asynchronous cells set as 1.0. The graph is representative of the results of four independent experiments.

(D) The GFP-TRAIP expressing cells were arrested at G1/S phase with a thymidine block (Thy) and released for 9 hours to synchronize them in late S phase with and without RO3306. The percentages of overlap between green (GFP-TRAIP) and blue (DNA) signals are indicated at the bottom of each image. The bar indicates 20 μm.

(E) GFP-TRAIP expressing cells were arrested at G1/S phase with a thymidine block, and then released for 9 hours to synchronize them in late S phase, in the absence or presence of RO3306. The percentages of overlap between GFP-TRAIP (green) fluorescence and endogenous PCNA immunofluorescence (cyan) in pre-extract treated cells are indicated at the right of the merged images. The bar indicates 5 μm.

(F) U2OS cells were arrested at G1/S phase with aphidicolin (aphi), and after release into S phase in the absence or presence of RO3306 were collected at the indicated times. The samples were

immunoblotted with the indicated antibodies. The protein levels of TRAIP in WCE and PCNA in the Chr fraction are quantified and indicated in the graph, relative to those in asynchronously growing cells set as 1.0.

Figure 4. TRAIP mediates the removal of chromatin-bound PCNA left after the induction of replication stress in mitotic cells.

(A) Endogenous PCNA immunofluorescence in asynchronously growing U2OS cells. The percentages of the cells with at least one PCNA signal (cyan) in mitotic chromatin are indicated at the bottom of each image. The bar indicates 10 μm.

(B) Asynchronously growing U2OS cells treated with 0.4μm aphidicolin or not, followed by the addition of EdU (green) to detect MiDAS. PCNA (cyan) was detected by immunofluorescence. The bar indicates 10 μm.

Figure 5. TRAIP is required for accurate cell cycle progression and appropriate cell growth

(A) Cell cycle profiles of asynchronously growing cells after depletion of the indicated proteins by RNAi. The ratios of cell populations at each cell cycle phase are indicated.

(B) Asynchronous (A) and mitosis-arrested (M) U2OS cells, depleted in the indicated proteins by RNAi or treated with the indicated drugs, were collected and divided into WCE and Chr factions, and immunoblotted with the indicated antibodies.

(C) Colony formation and cell growth assays of U2OS cells with depletion of the indicated proteins.

(D) TRAIP-mAID expressing cells were collected at the indicated times after the addition of auxin (5-ph-IAA). WCE and Chr fractions were prepared and immunoblotted with the indicated antibodies.

(E) The graph shows the ratios of cell cycle phases of asynchronously growing cells after the addition of auxin, based on the cell cycle profiles indicated at the right.

Figure 6. TRAIP is required for precise mitotic progression and exit, and faithful S phase entry

(A) The ratios of cell cycle phases of cells arrested in mitosis and released in the absence or presence of auxin, based on the cell cycle profiles indicated at the right. The graph is representative of the results of four independent experiments and the averages of each ratio are shown.

(B) The WCE and Chr fractions of the same cell samples collected in (A) were immunoblotted with the indicated antibodies.

(C) Asynchronous TRAIP-mAID expressing cells grown in the absence or presence of auxin were immunostained with anti-Cdt1 antibody (cyan), after pre-extract treatment. S phase cells were detected by observing EdU incorporation (green). The percentages of Cdt1 signals detected in S phase, mitosis, and G2 or G1 phase are indicated at the right of the images. The bar indicates 5 μm.

Fig1A

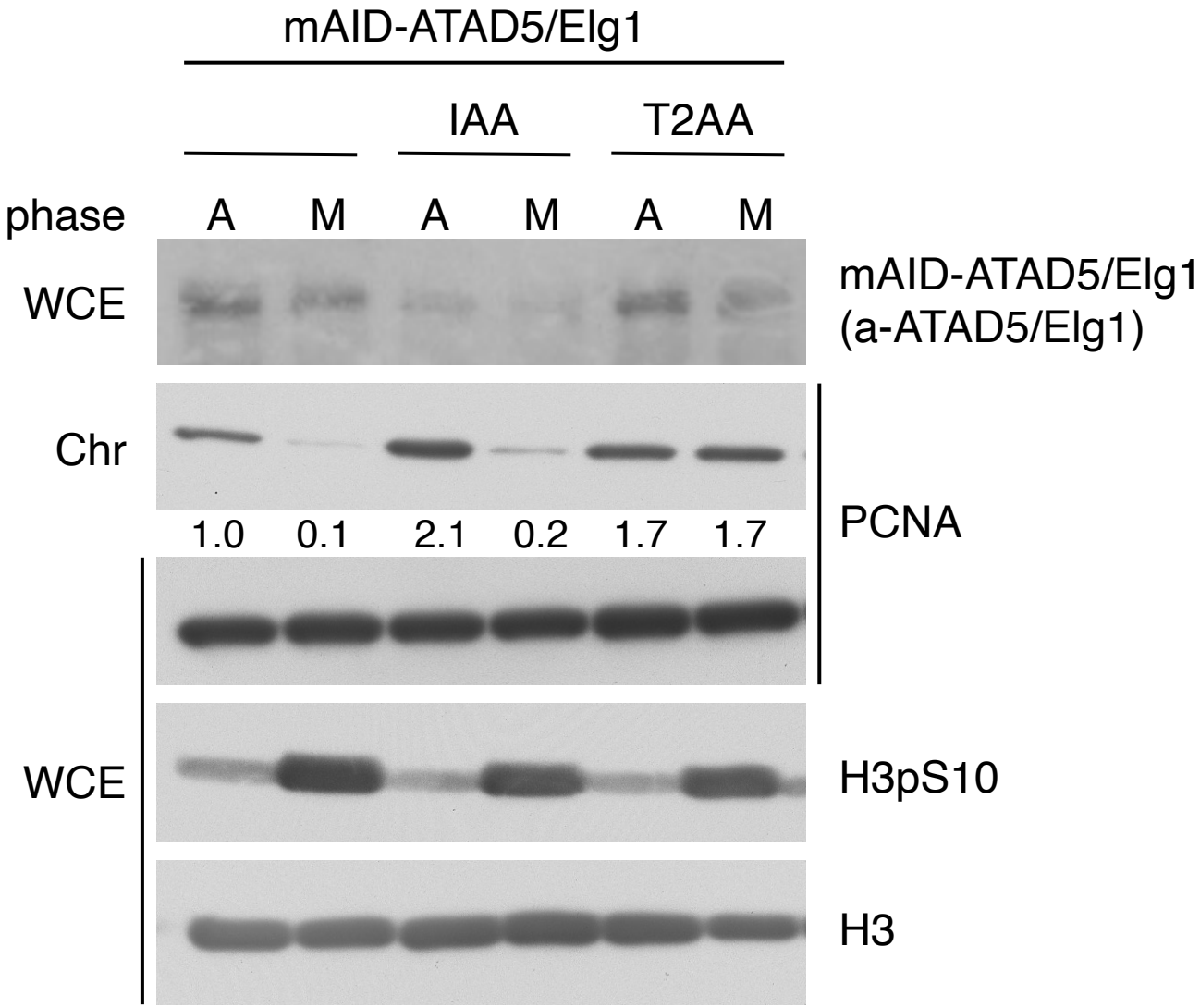
mAID-ATAD5/Elg1
IAA
T2AA
phase
A
M
A
M
A
M
WCE
mAID-ATAD5/Elg1
(a-ATAD5/Elg1)
Chr
1.0
0.1
2.1
0.2
1.7
1.7
PCNA
WCE
H3pS10
H3

Fig1B

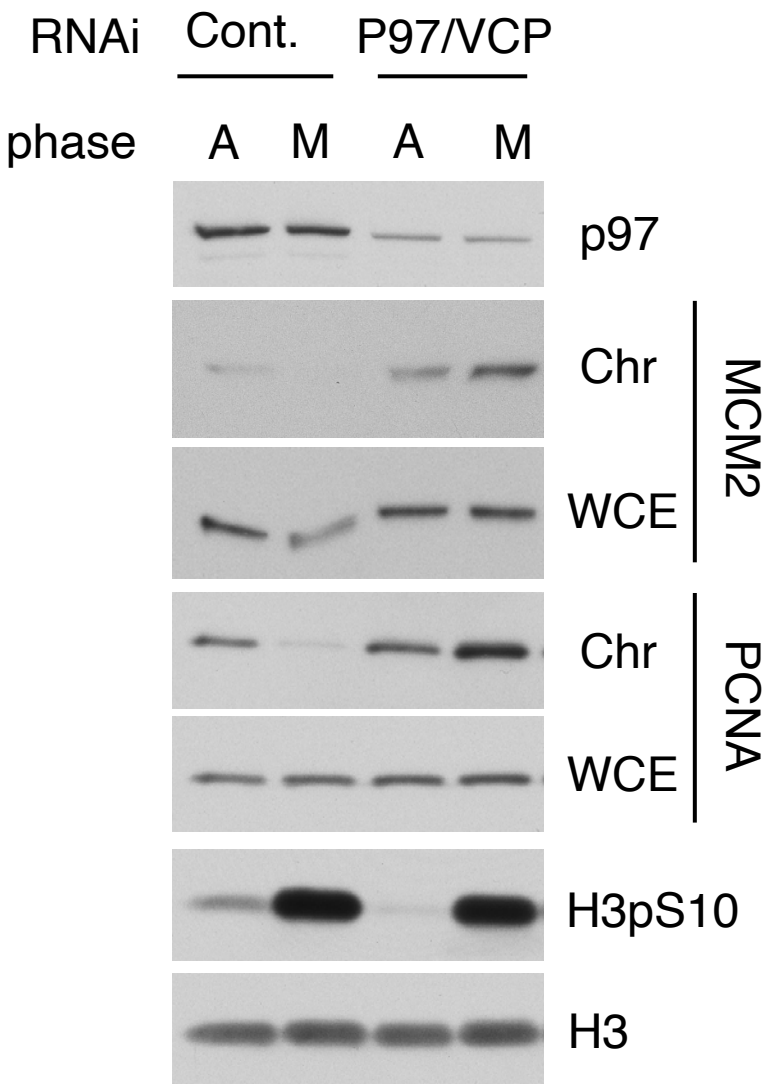
RNAi
Cont.
P97/VCP
phase
A
M
A
M
p97
Chr
WCE
MCM2
Chr
WCE
PCNA
H3pS10
H3

Fig1C

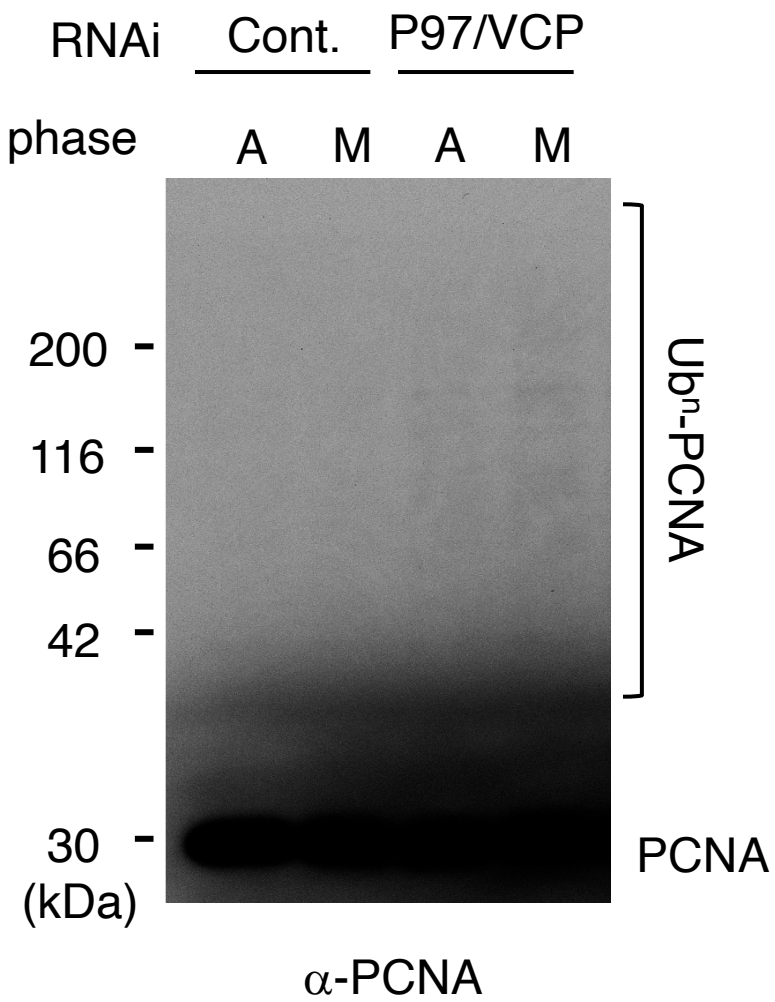
RNAi
Cont.
P97/VCP
phase
A
M
A
M
200
116
66
42
30
(kDa)
Ubⁿ-PCNA
PCNA
α-PCNA

Fig1D

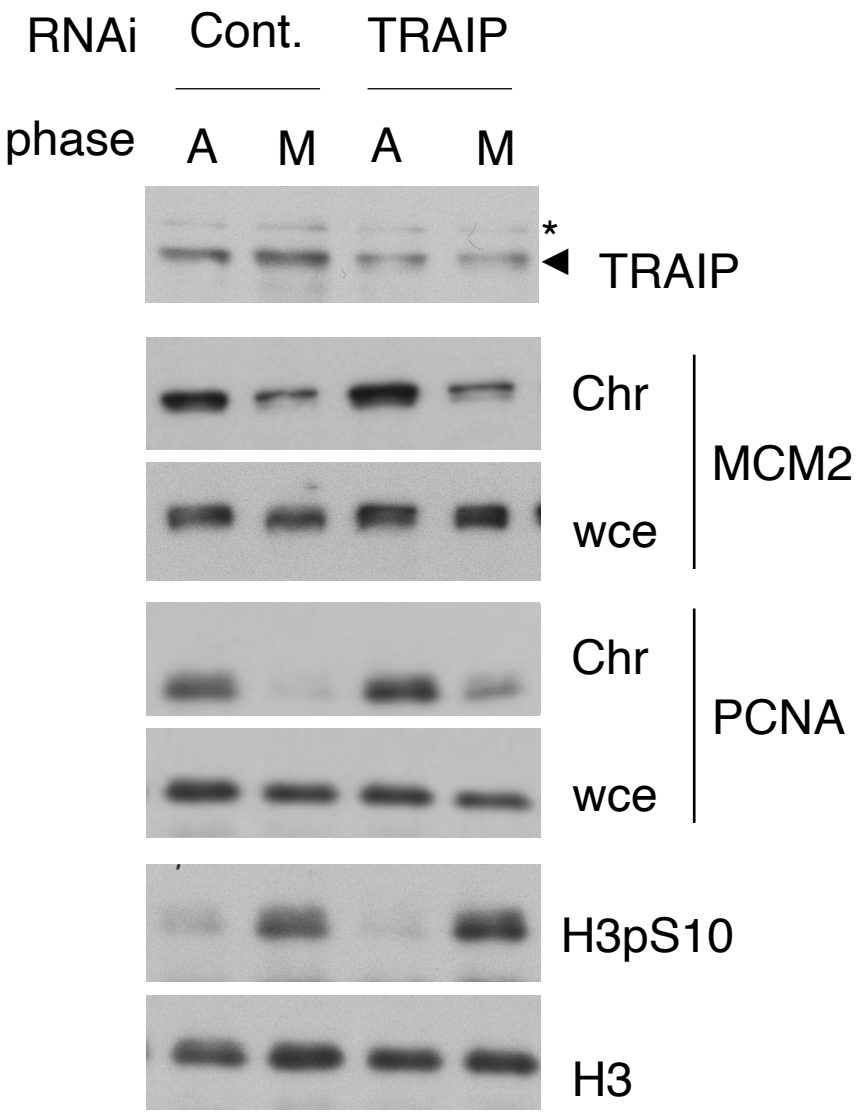
RNAi
Cont.
TRAIP
phase
A
M
A
M
*
TRAIP
Chr
wce
MCM2
Chr
wce
PCNA
H3pS10
H3

Fig1E

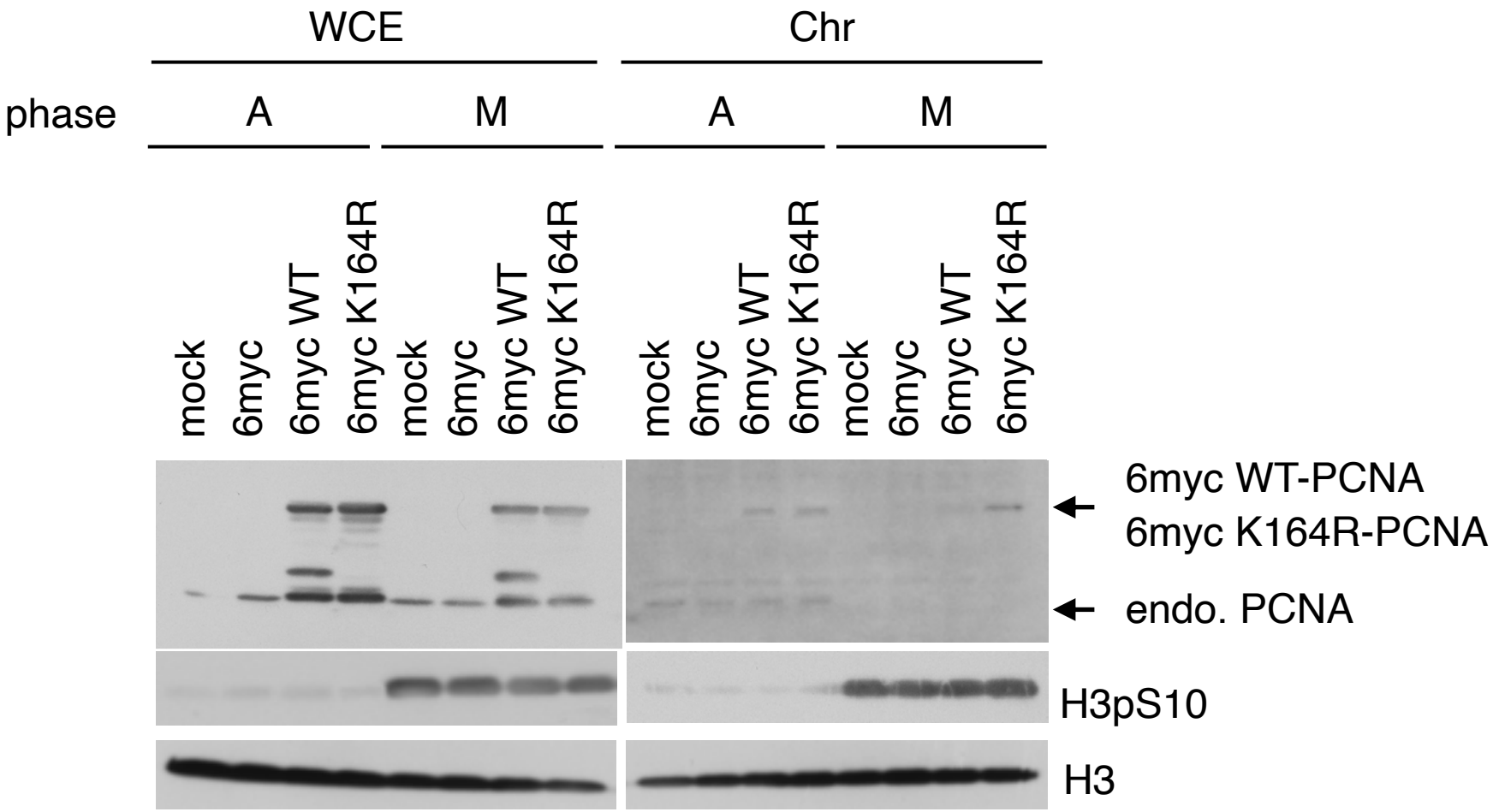
WCE
Chr
phase
A
M
A
M
mock
6myc
6myc WT
6myc K164R
mock
6myc
6myc WT
6myc K164R
mock
6myc
6myc WT
6myc K164R
mock
6myc
6myc WT
6myc K164R
6myc WT-PCNA
6myc K164R-PCNA
endo. PCNA
H3pS10
H3

Fig2A

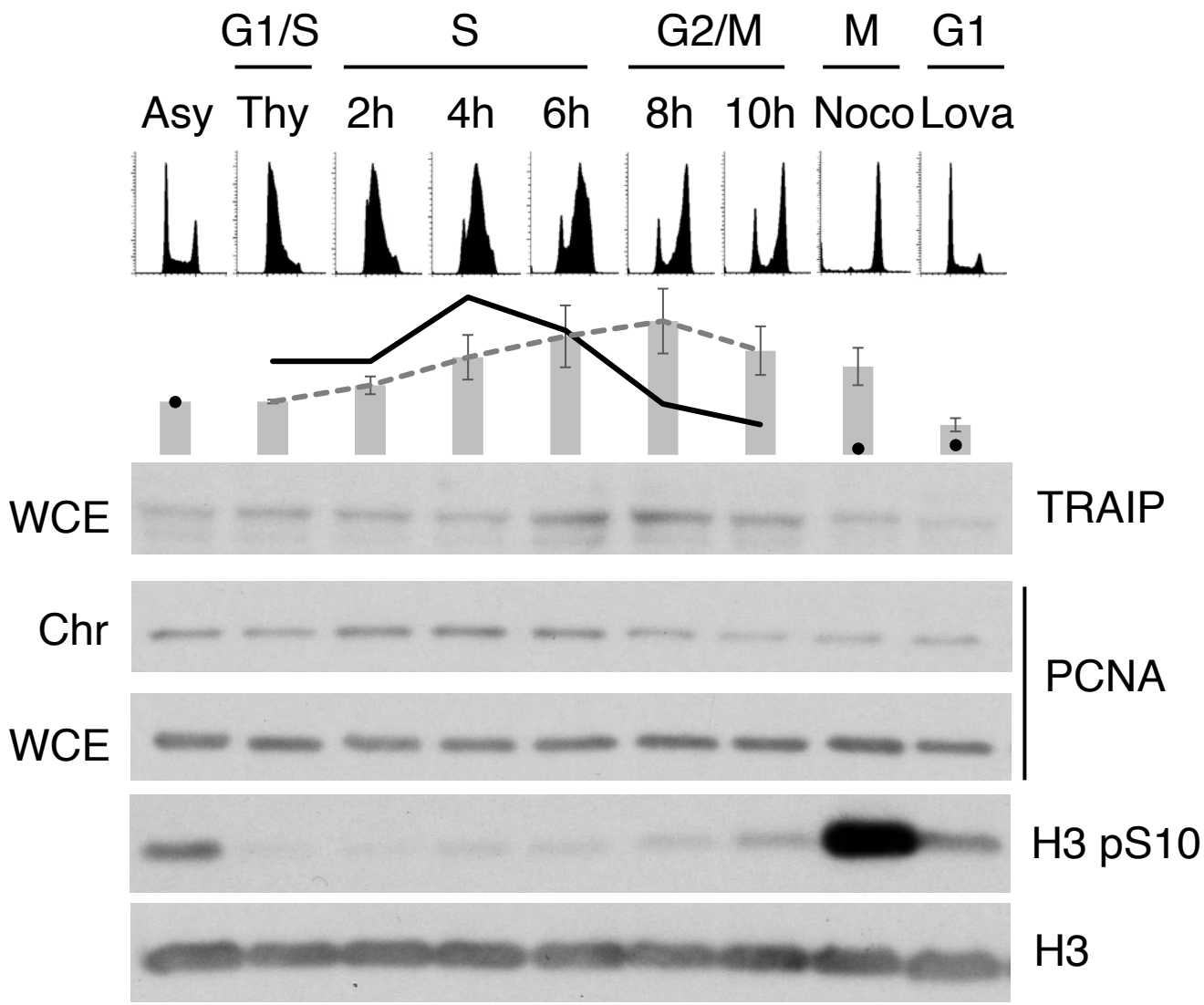
G1/S
S
G2/M
M
G1
Asy
Thy
2h
4h
6h
8h
10h
Noco
Lova
WCE
TRAIP
Chr
PCNA
WCE
H3 pS10
H3

Fig2B

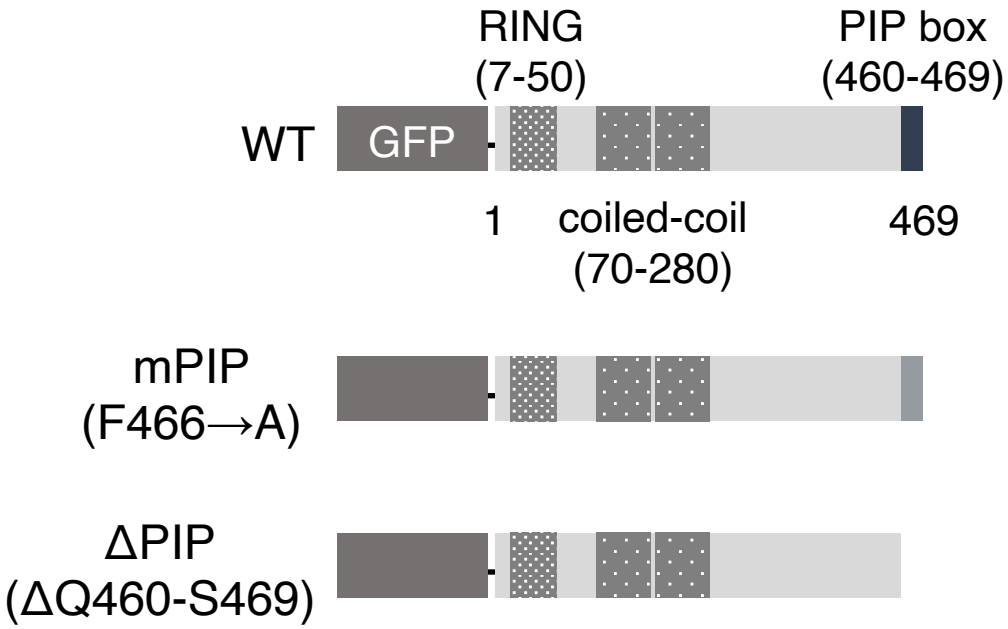
RING
(7-50)
PIP box
(460-469)
WT
GFP
1
coiled-coil
(70-280)
469
mPIP
(F466→A)
ΔPIP
(ΔQ460-S469)

Fig2C

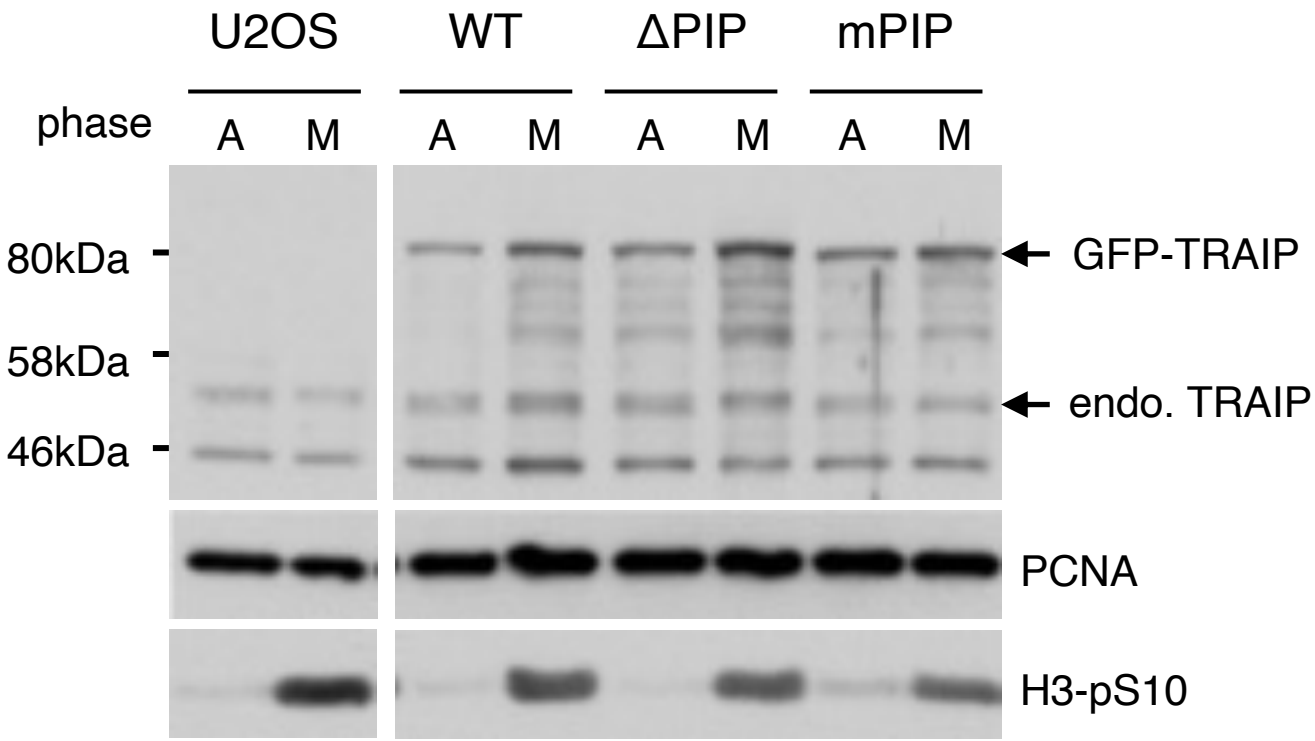
U2OS
WT
ΔPIP
mPIP
phase
A
M
A
M
A
M
A
M
80kDa
58kDa
46kDa
GFP-TRAIP
endo. TRAIP
PCNA
H3-pS10

Fig2D

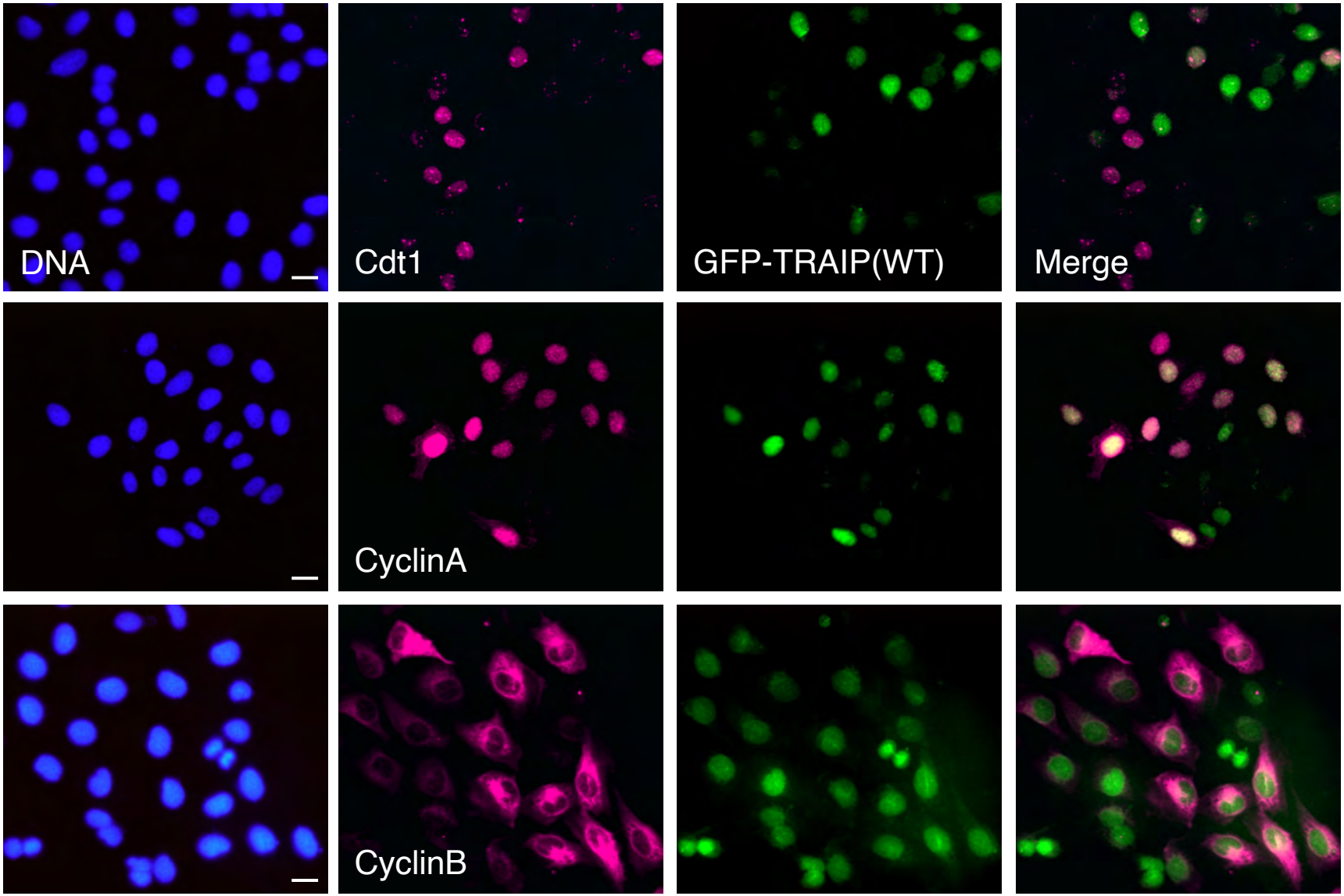

14.0%
(n=315)

58.7%
(n=300)

73.0%
(n=74)

Fig2E

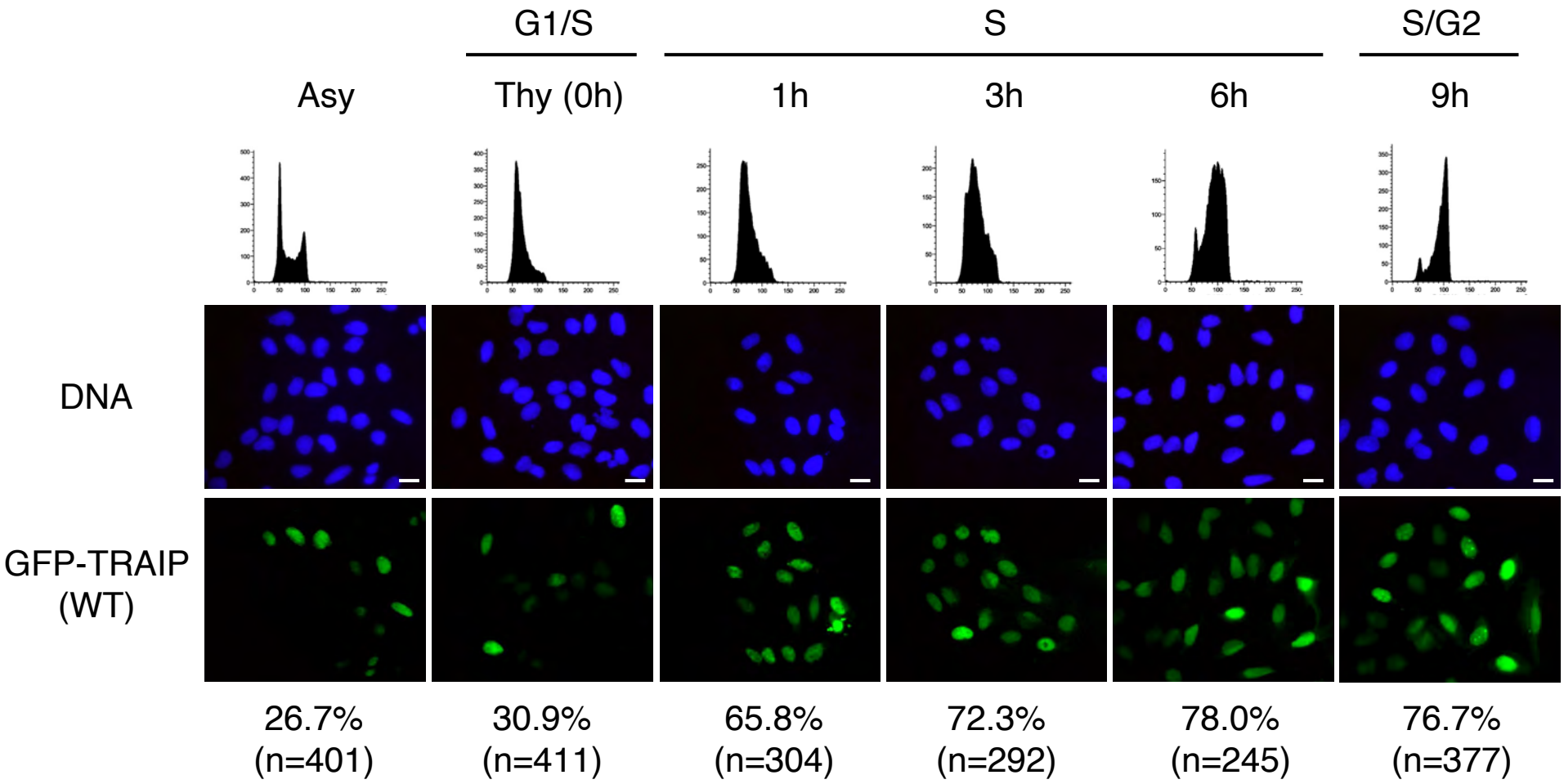
G1/S
S
S/G2
Asy
Thy (0h)
1h
3h
6h
9h
DNA
GFP-TRAIP
(WT)
26.7%
(n=401)
30.9%
(n=411)
65.8%
(n=304)
72.3%
(n=292)
78.0%
(n=245)
76.7%
(n=377)

Fig2F

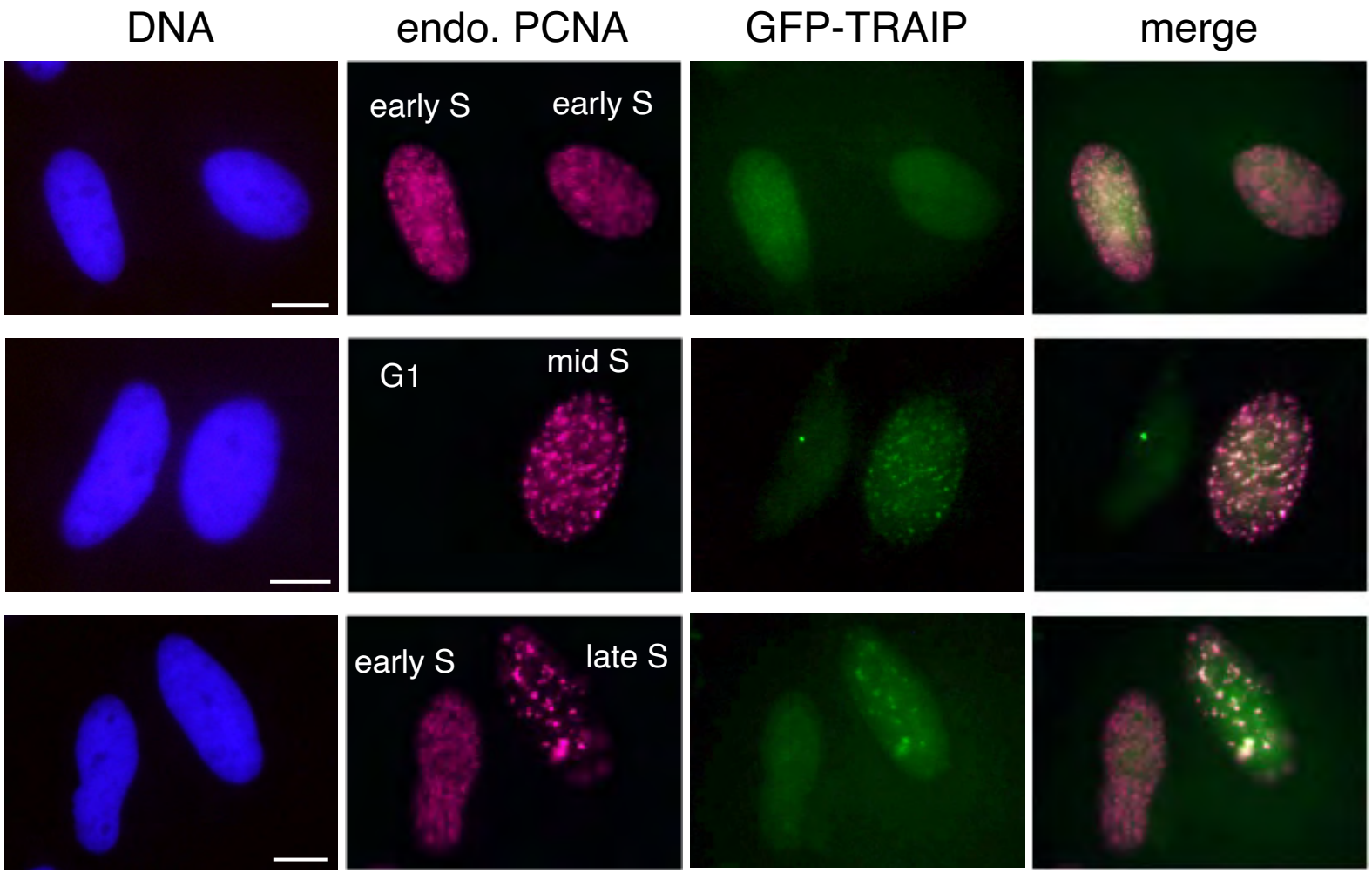
DNA
endo. PCNA
GFP-TRAIP
merge
early S
early S
G1
mid S
early S
late S

Fig3A

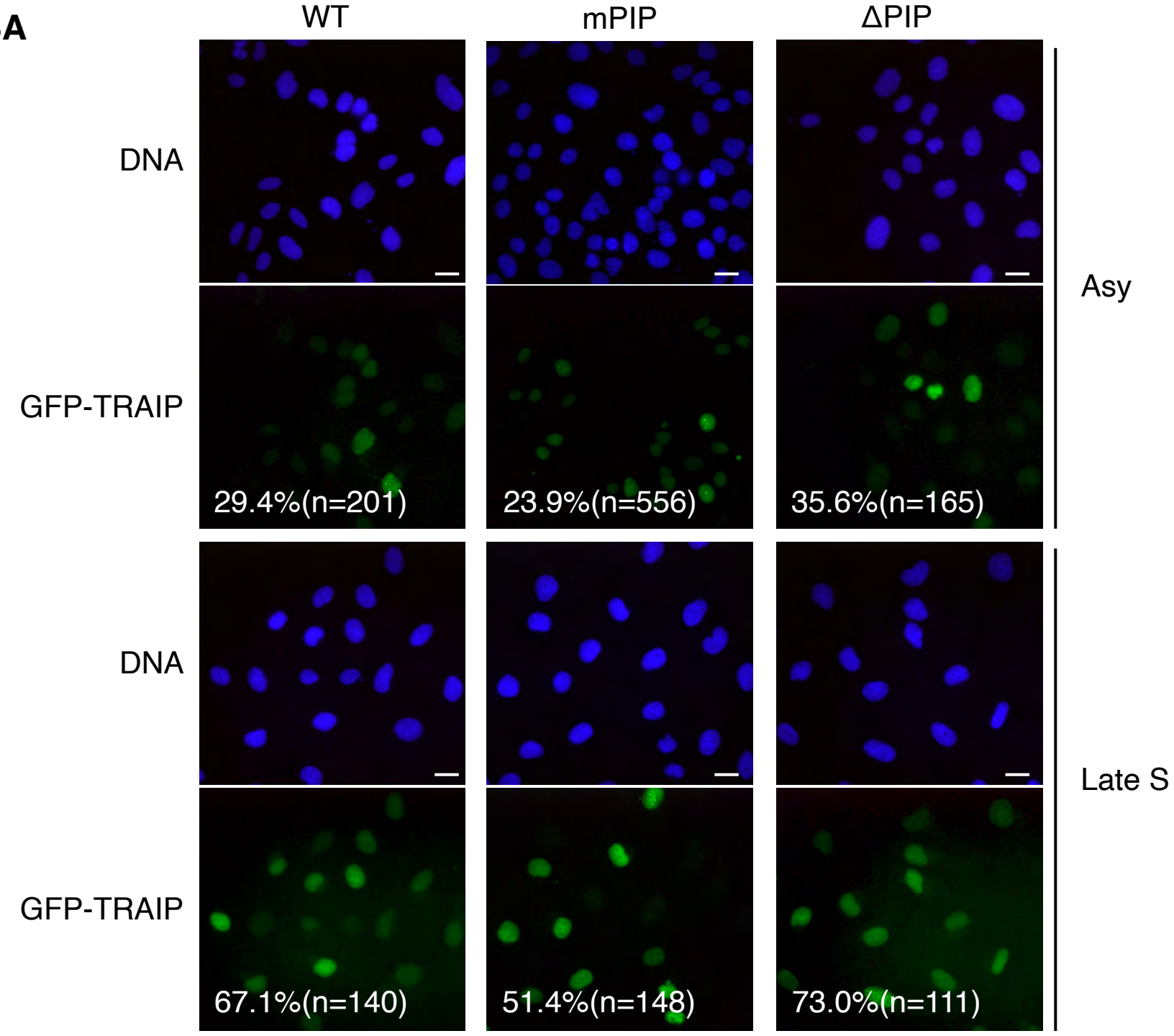
WT
mPIP
ΔPIP
DNA
GFP-TRAIP
29.4%(n=201)
23.9%(n=556)
35.6%(n=165)
Asy
DNA
GFP-TRAIP
67.1%(n=140)
51.4%(n=148)
73.0%(n=111)
Late S

Fig3B

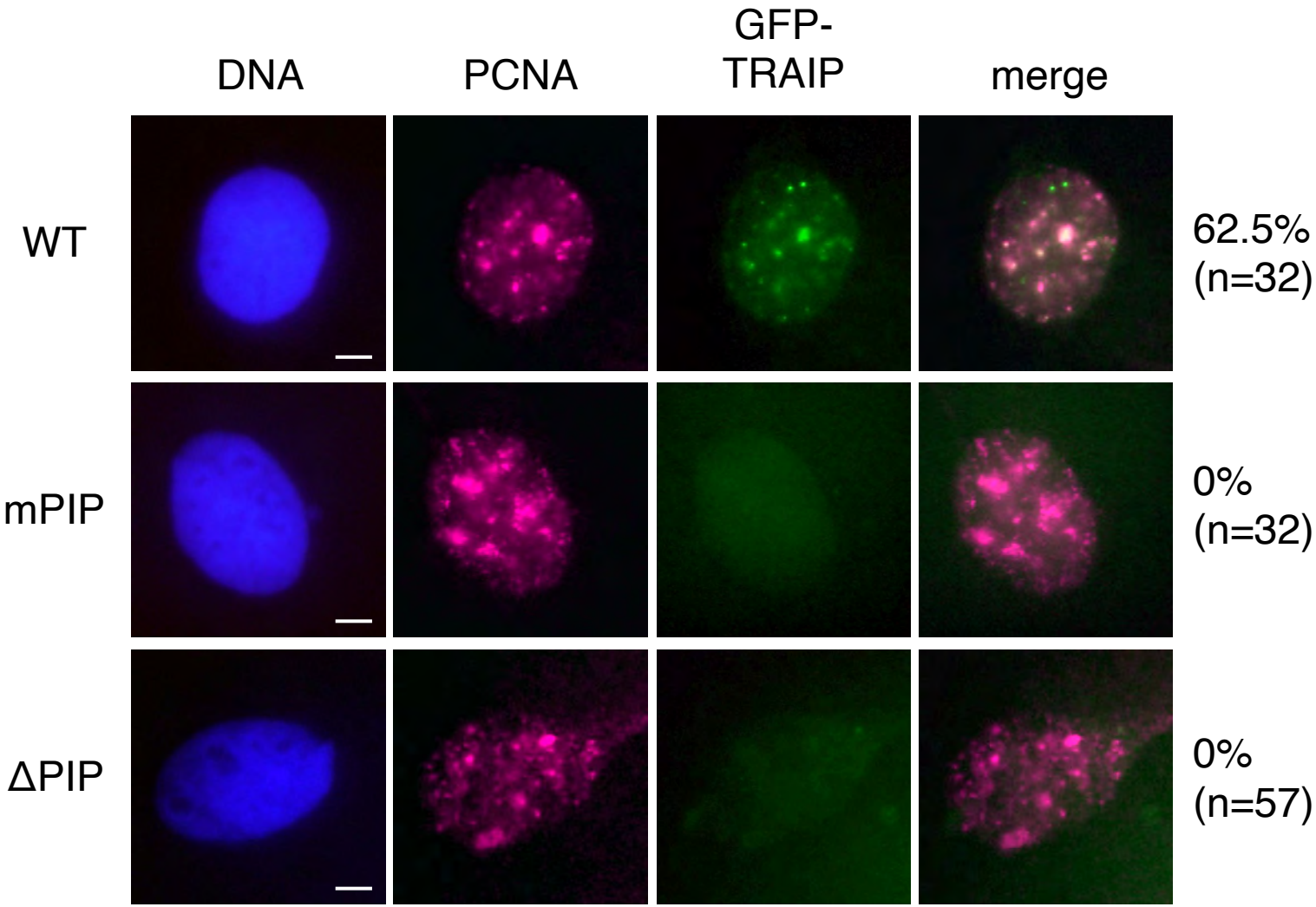

Fig3C

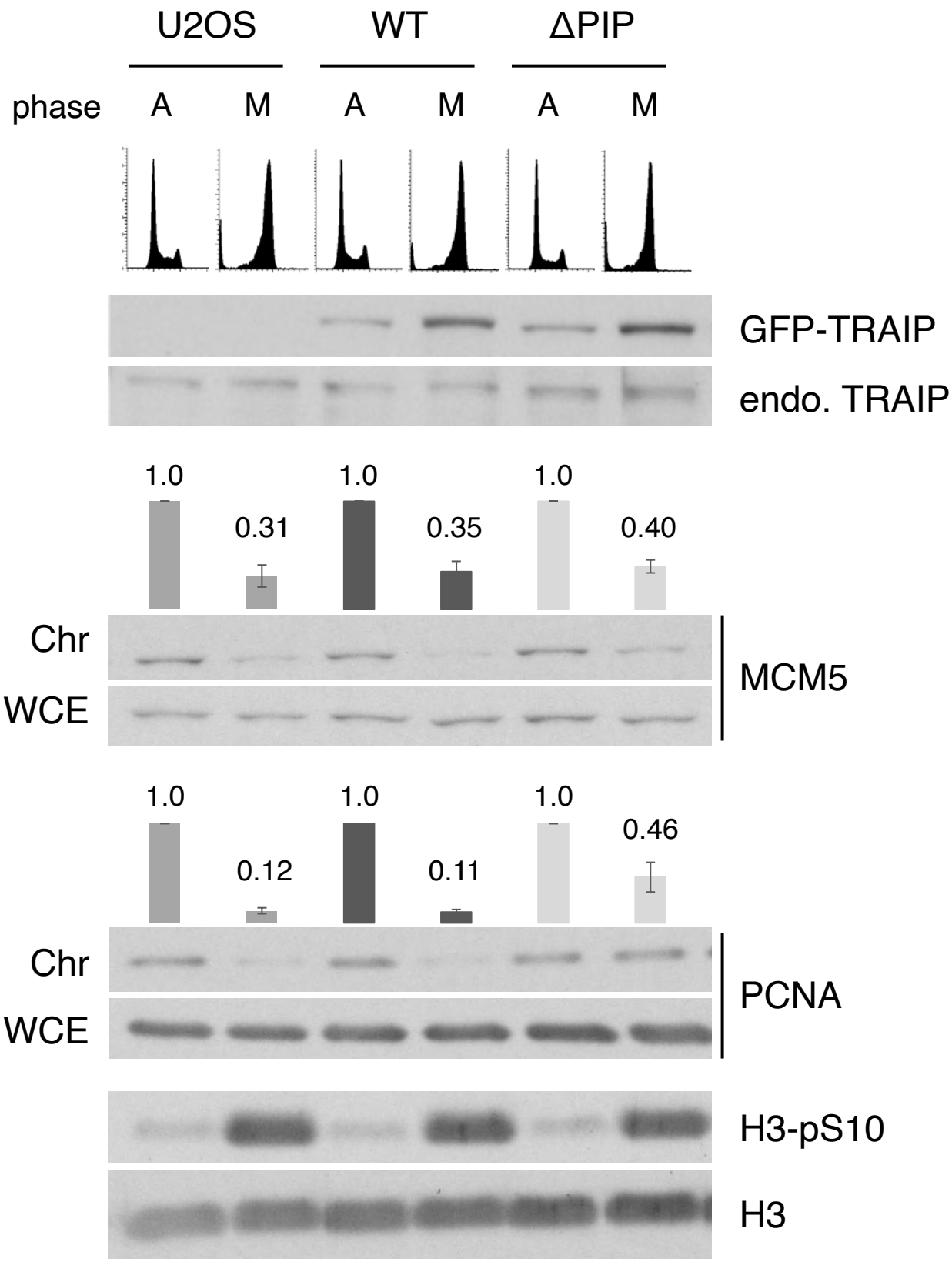
U2OS
WT
ΔPIP
phase
A
M
A
M
A
M
GFP-TRAIP
endo. TRAIP
1.0
0.31
1.0
0.35
1.0
0.40
Chr
WCE
MCM5
1.0
0.12
1.0
0.11
1.0
0.46
Chr
WCE
PCNA
H3-pS10
H3

Fig3D

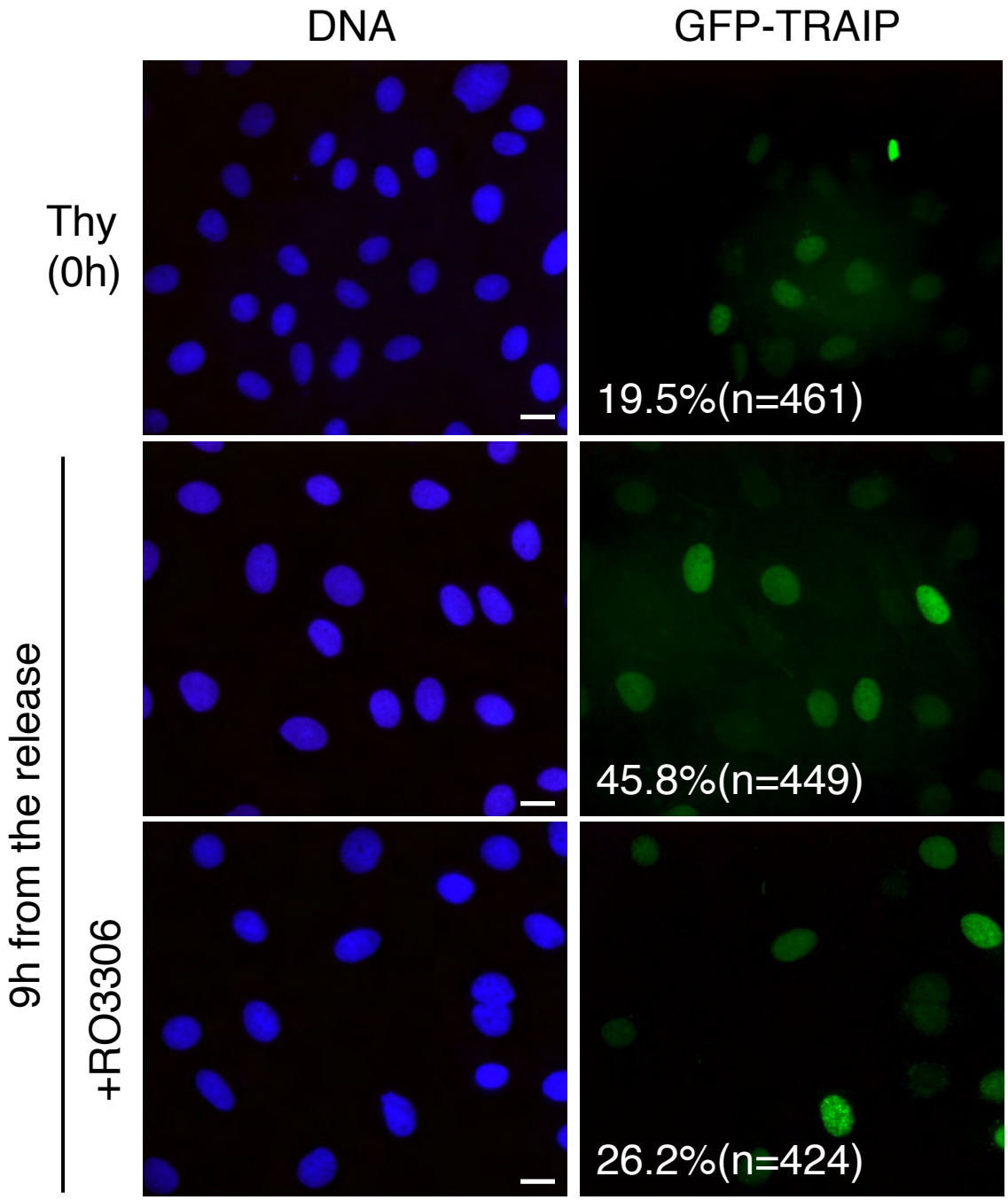
DNA
GFP-TRAIP
Thy
(0h)
19.5%(n=461)
9h from the release
45.8%(n=449)
+RO3306
26.2%(n=424)

Fig3E

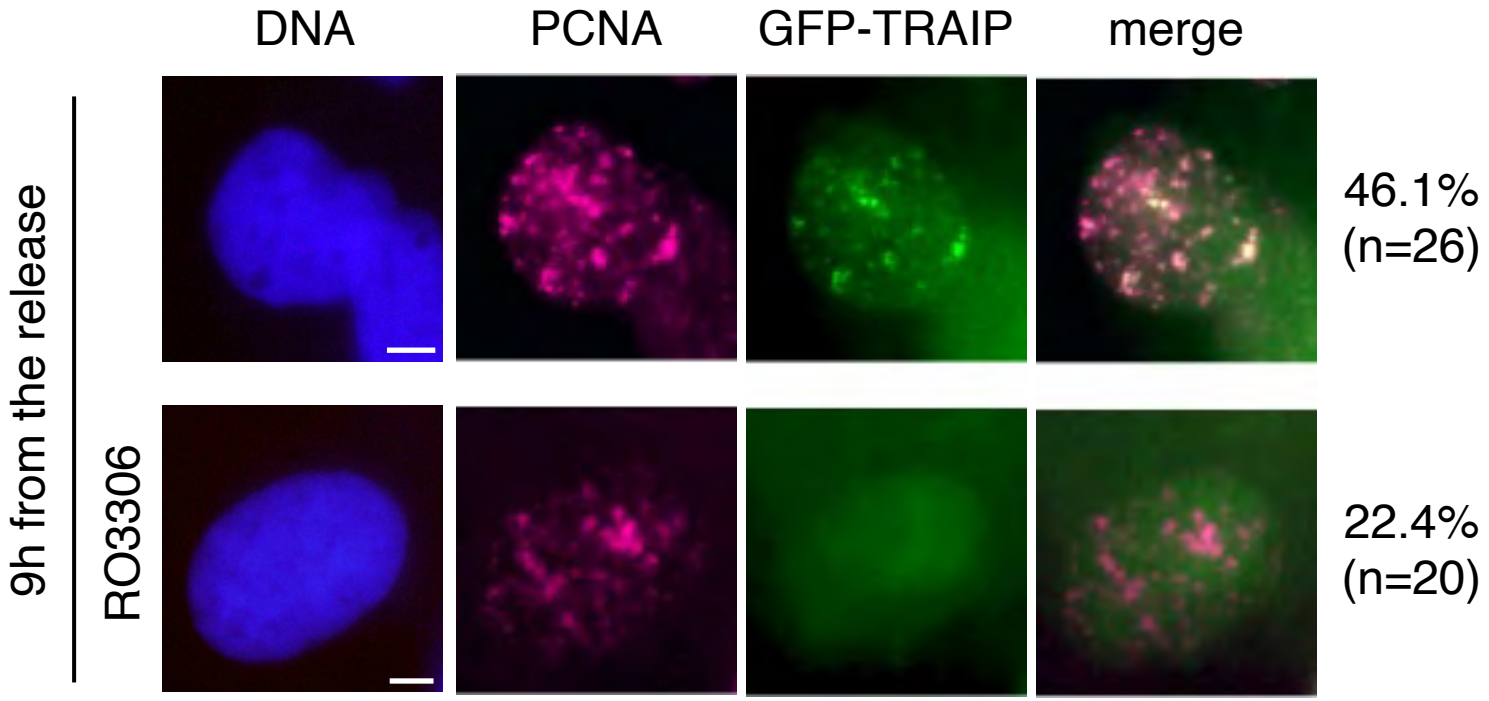
DNA
PCNA
GFP-TRAIP
merge
9h from the release
RO3306
46.1%
(n=26)
22.4%
(n=20)

Fig3F

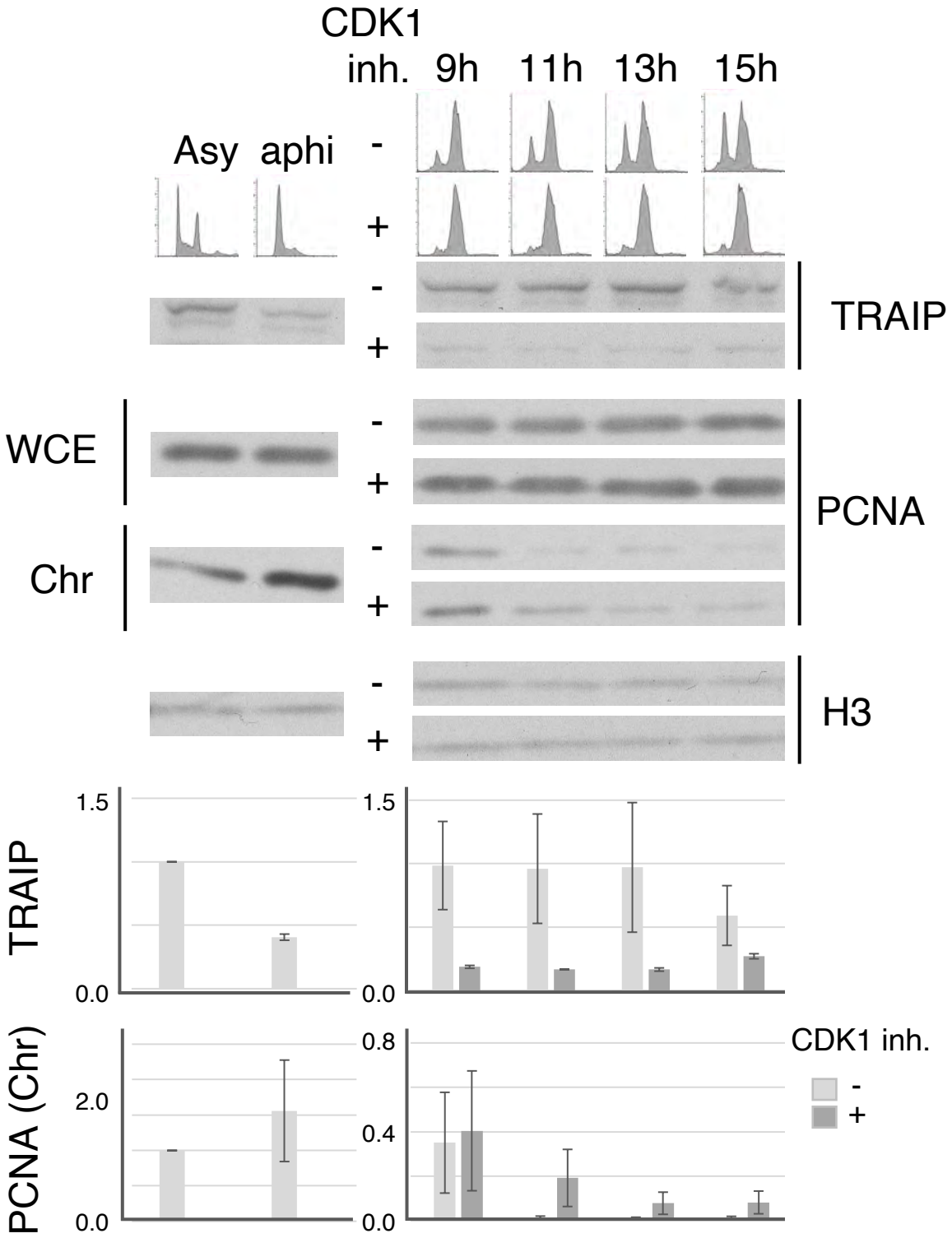
CDK1 inh.
9h
11h
13h
15h
Asy
aphi
-
+
TRAIP
WCE
Chr
PCNA
H3
TRAIP
PCNA (Chr)
1.5
0.0
2.0
0.8
0.4
CDK1 inh.
-
+

Fig4A

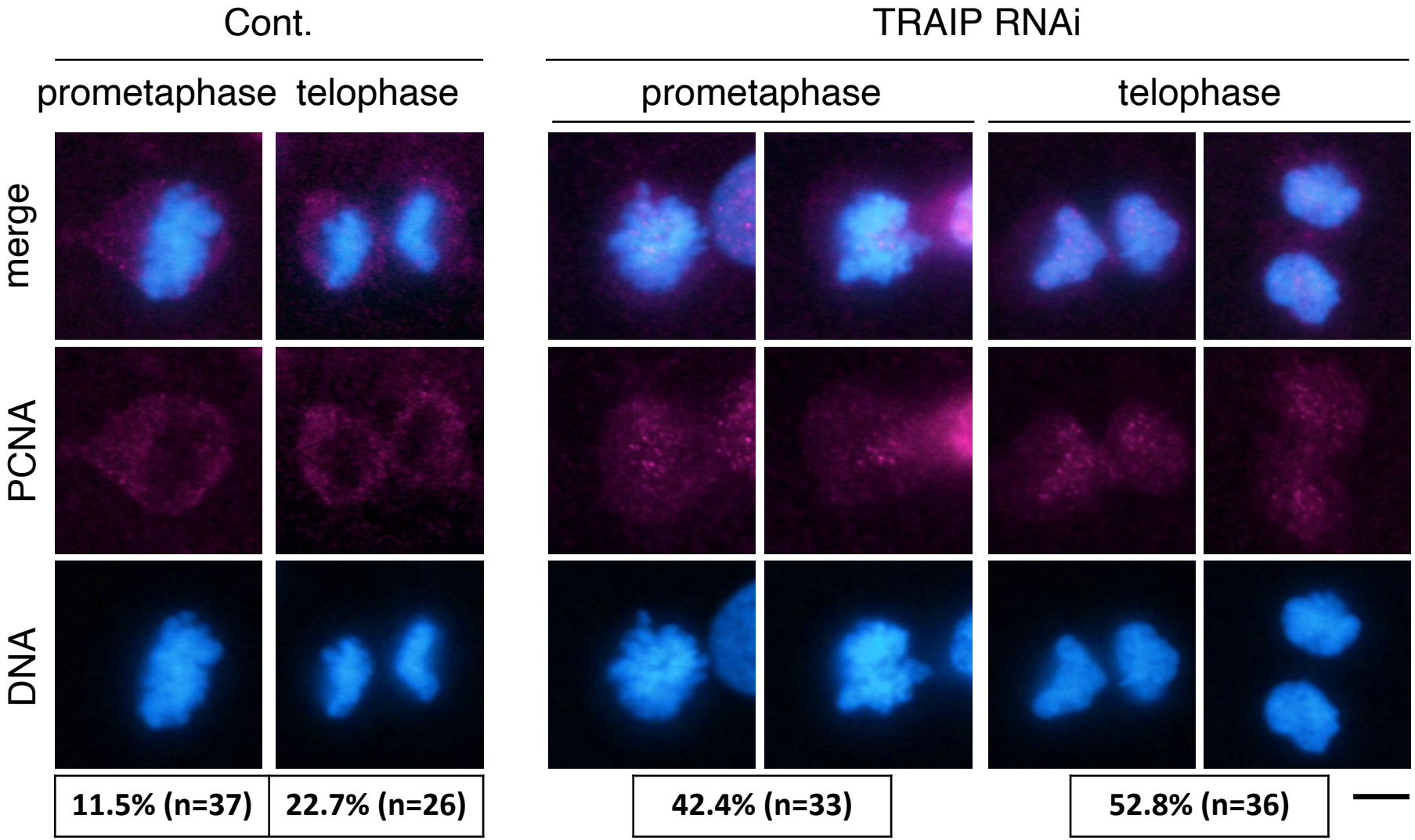
Cont.
TRAIP RNAi
prometaphase
telophase
prometaphase
telophase
merge
PCNA
DNA
11.5% (n=37)
22.7% (n=26)
42.4% (n=33)
52.8% (n=36)

Fig4B

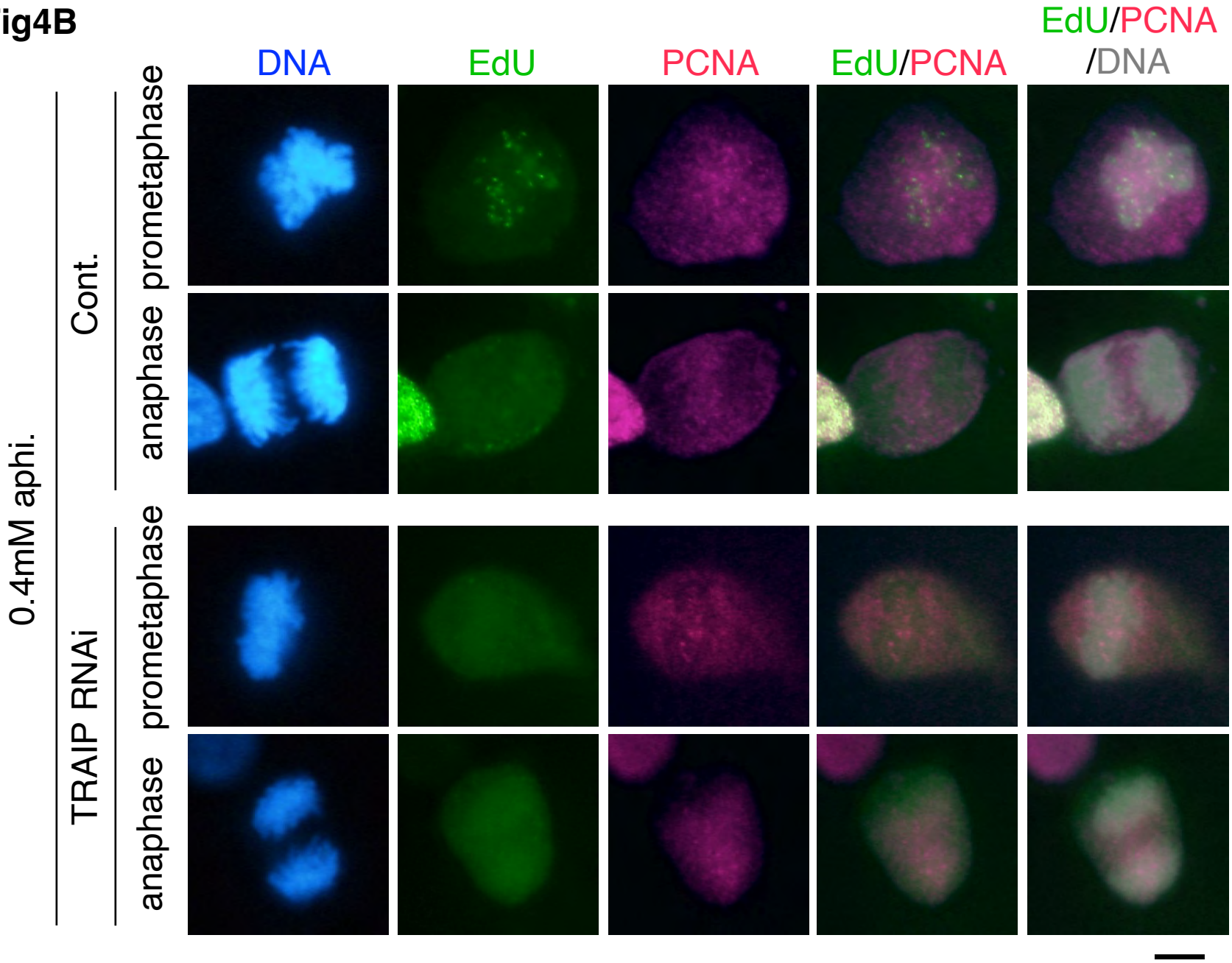
DNA
EdU
PCNA
EdU/PCNA
EdU/PCNA
/DNA
0.4mM aphi.
Cont.
TRAIP RNAi
prometaphase
anaphase
prometaphase
anaphase

Fig5A

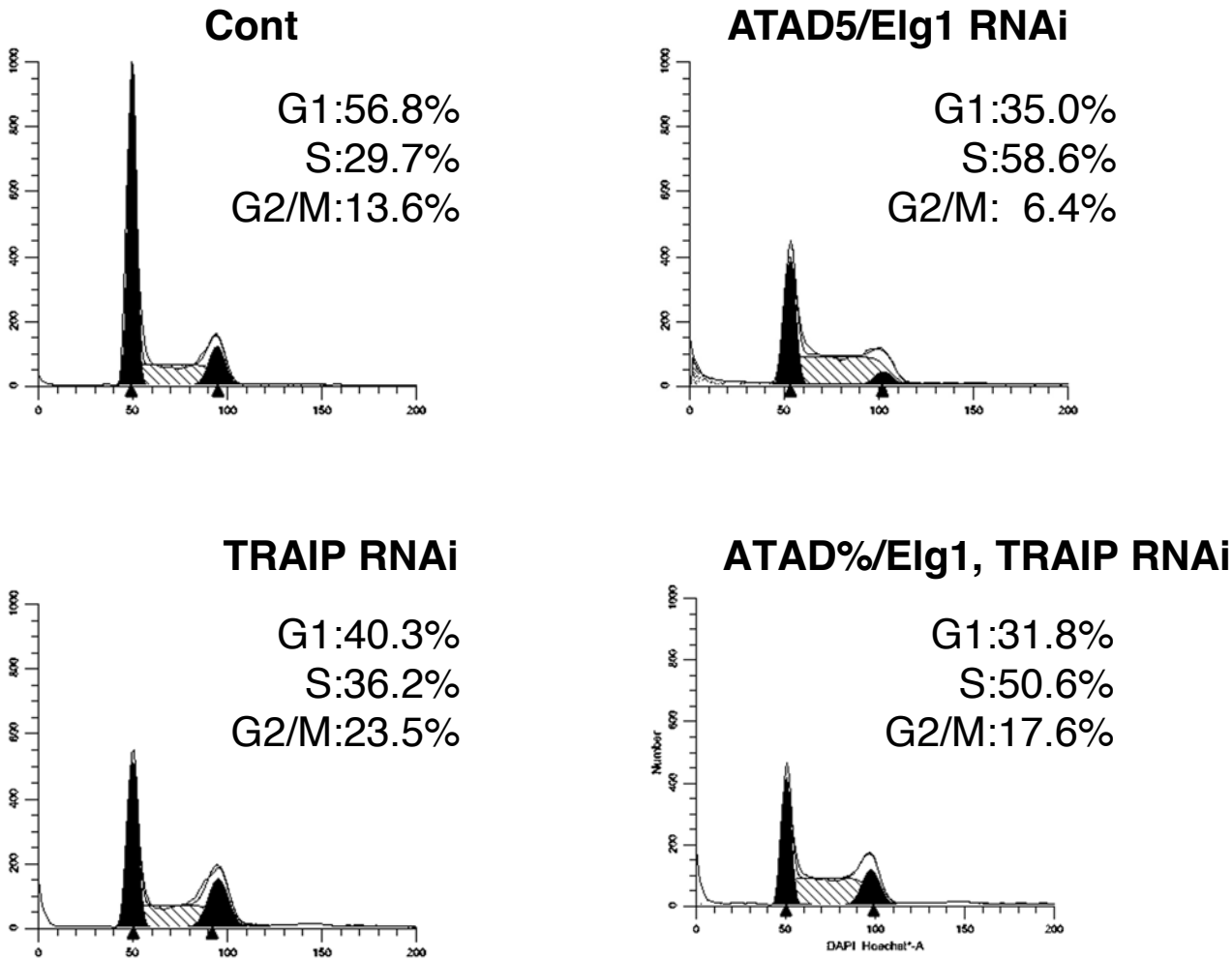
Cont
G1:56.8%
S:29.7%
G2/M:13.6%
ATAD5/Elg1 RNAi
G1:35.0%
S:58.6%
G2/M: 6.4%
TRAIP RNAi
G1:40.3%
S:36.2%
G2/M:23.5%
ATAD%/Elg1, TRAIP RNAi
G1:31.8%
S:50.6%
G2/M:17.6%
Number
DAPI Hoechst*-A

Fig5B

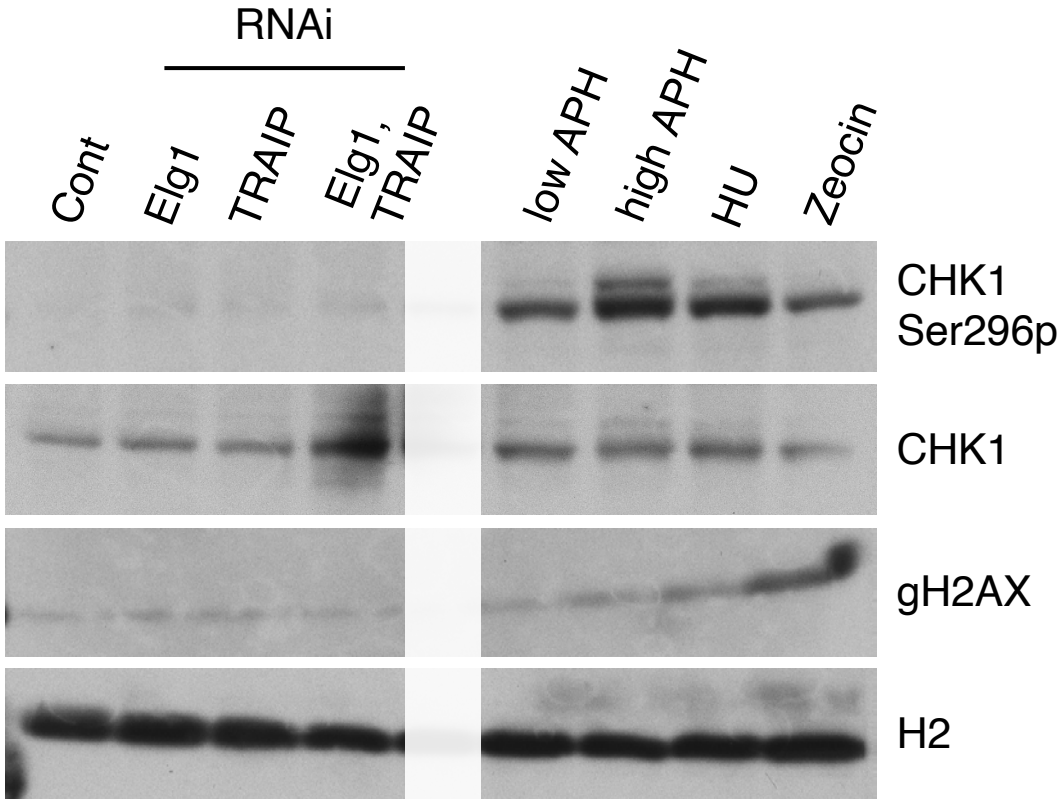
RNAi
Cont
Elg1
TRAIP
Elg1, TRAIP
low APH
high APH
HU
Zeocin
CHK1 Ser296p
CHK1
gH2AX
H2

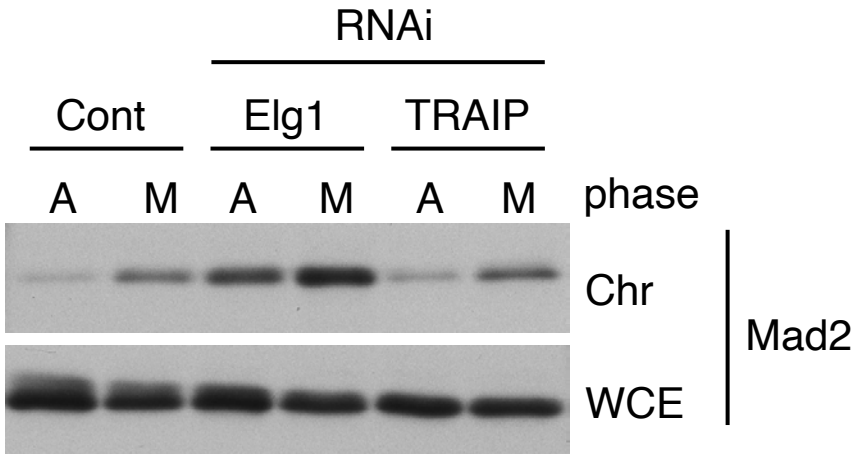
RNAi
Cont
Elg1
TRAIP
A
M
A
M
A
M
phase
Chr
WCE
Mad2

Fig5C

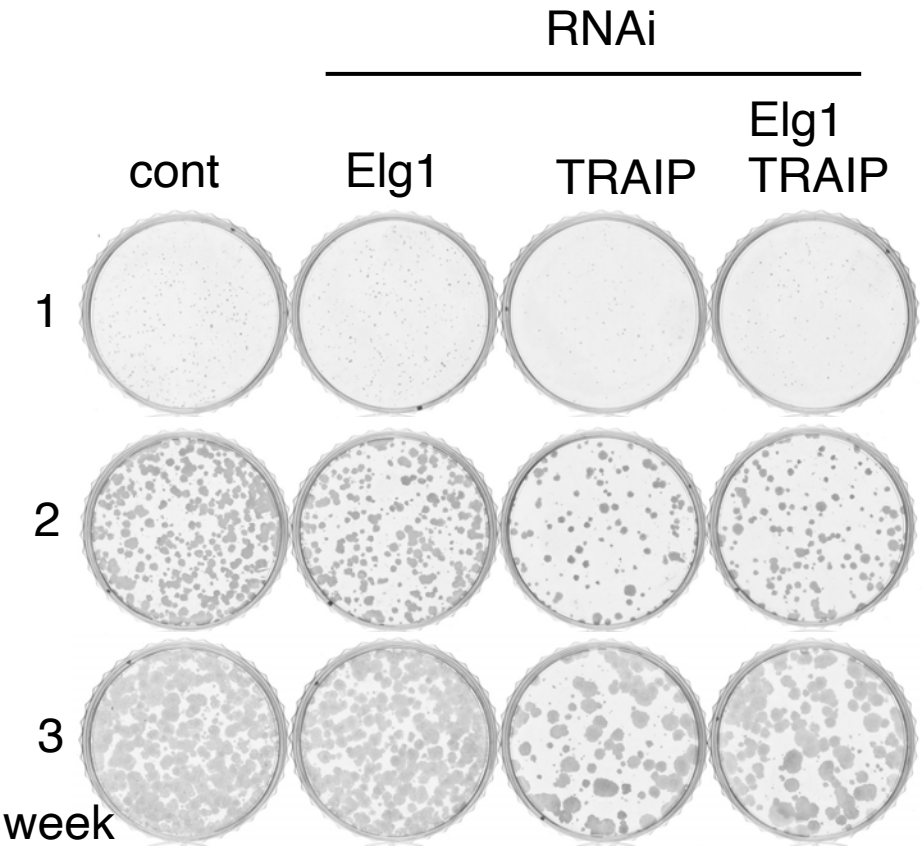
RNAi
cont
Elg1
TRAIP
Elg1
TRAIP
1
2
3
week

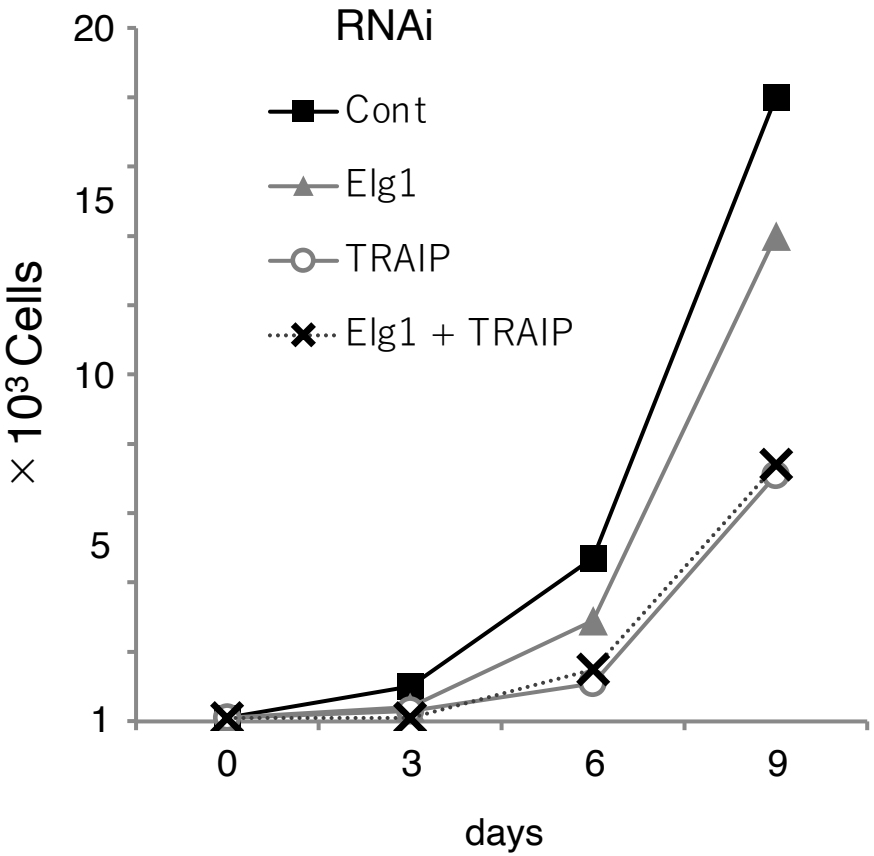
RNAi
Cont
Elg1
TRAIP
Elg1 + TRAIP
× 10³ Cells
20
15
10
5
1
0
3
6
9
days

Fig5D

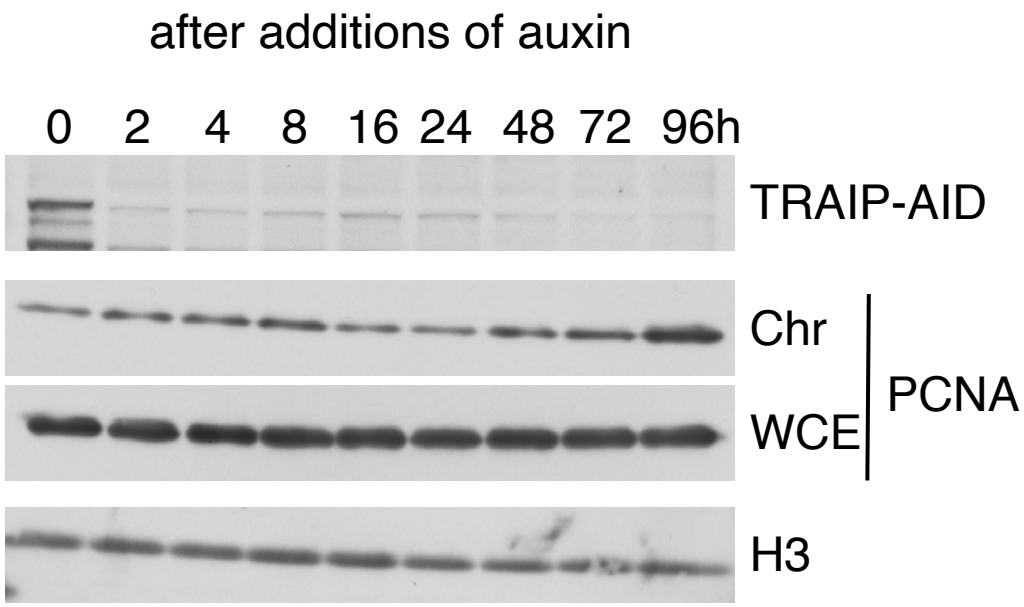
after additions of auxin
0
2
4
8
16
24
48
72
96h
TRAIP-AID
Chr
WCE
PCNA
H3

Fig5E

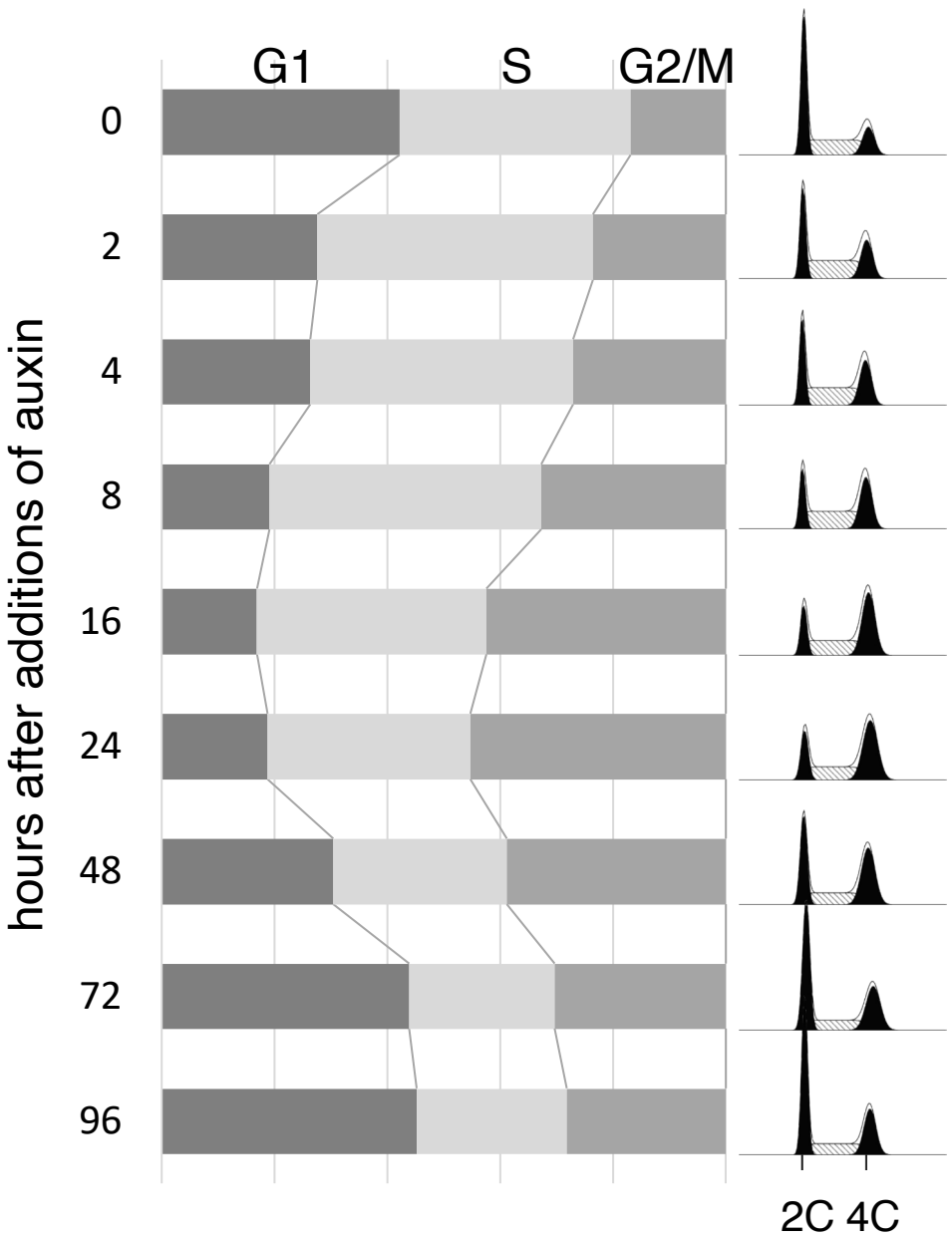
G1
S
G2/M
hours after additions of auxin
0
2
4
8
16
24
48
72
96
2C
4C

Fig6A

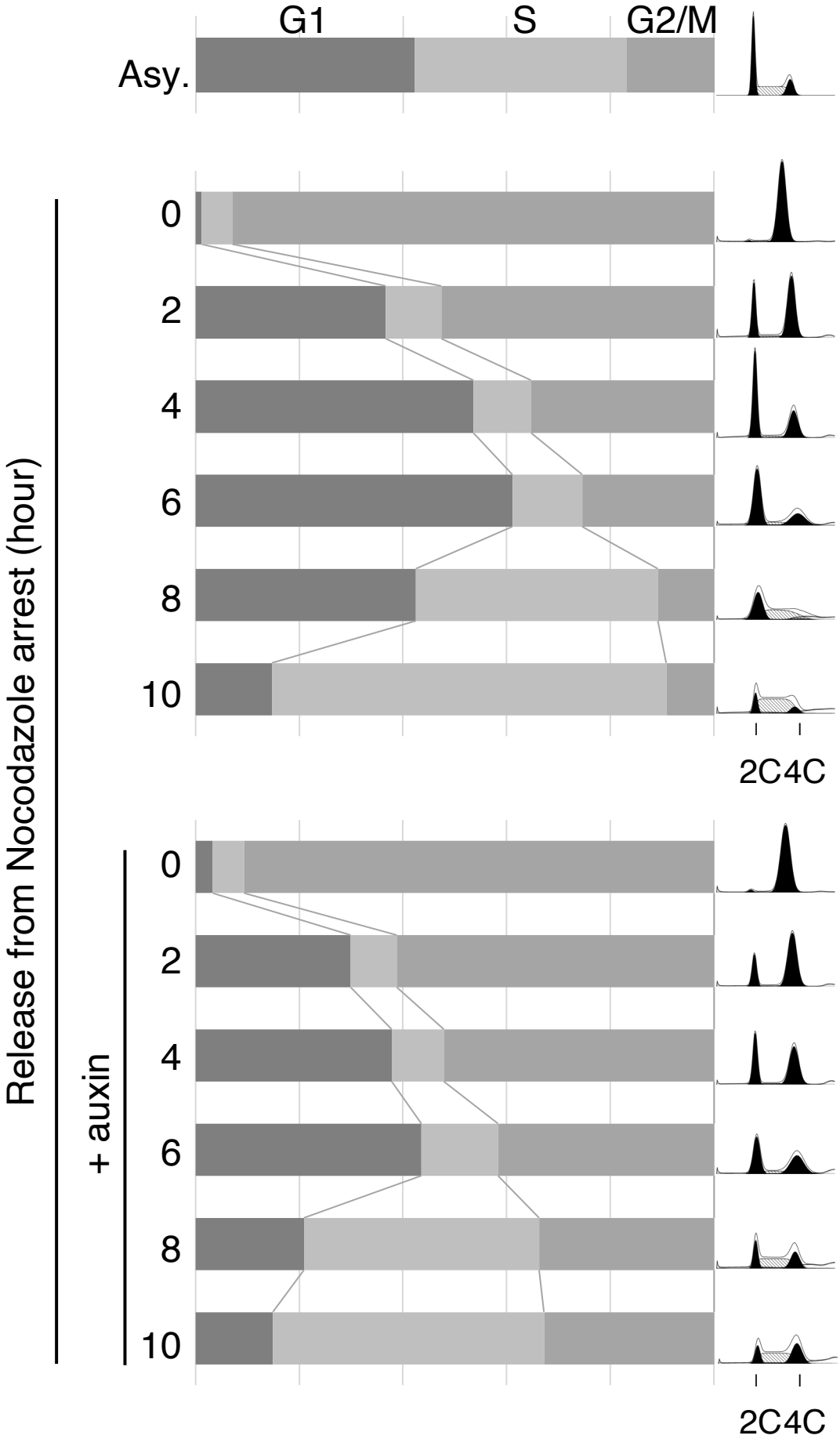
G1
S
G2/M
Asy.
0
2
4
6
8
10
2C4C
Release from Nocodazole arrest (hour)
+ auxin
0
2
4
6
8
10
2C4C

Fig6B

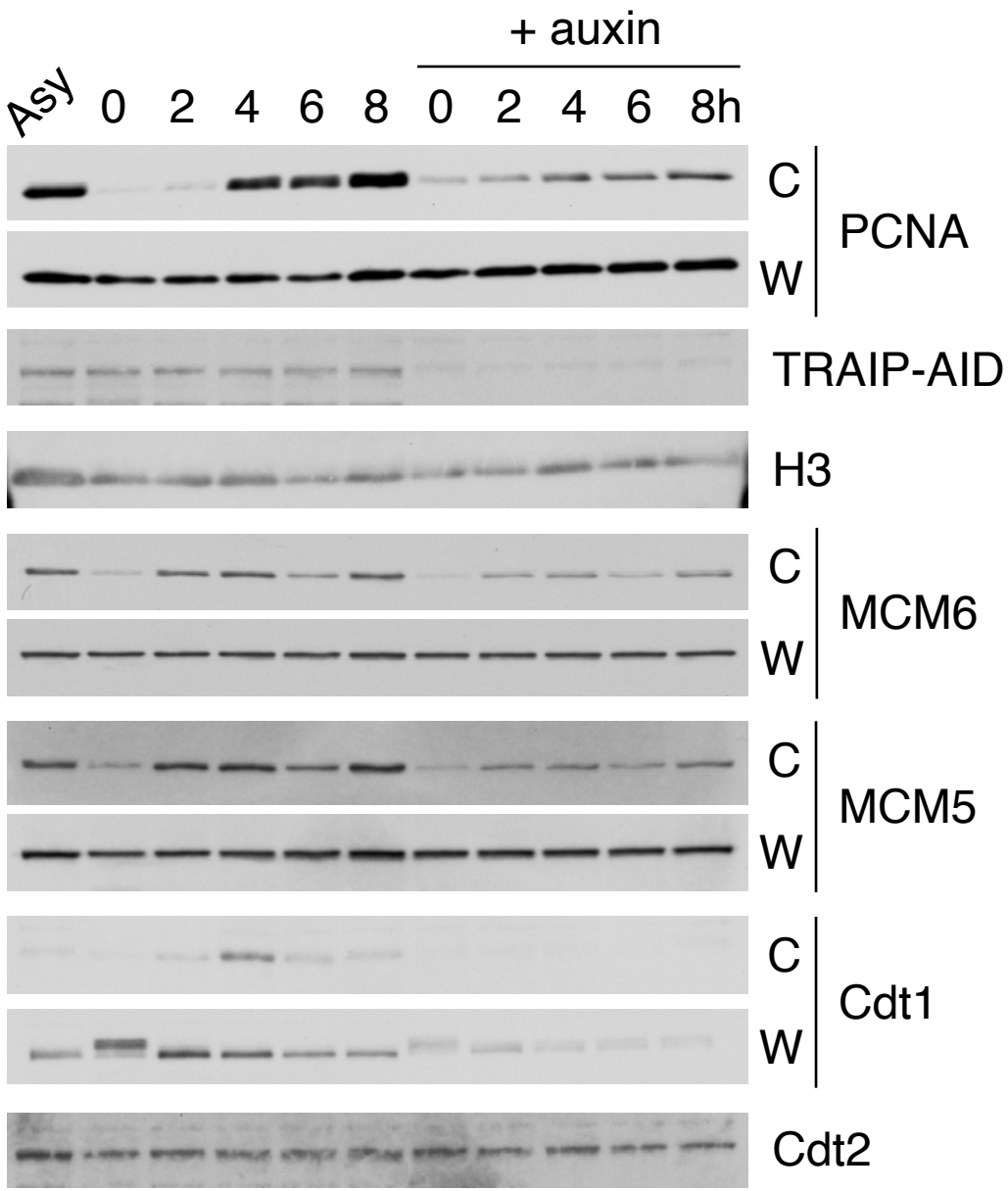
+ auxin
Asy
0
2
4
6
8
0
2
4
6
8h
C
W
PCNA
TRAIP-AID
H3
C
W
MCM6
C
W
MCM5
C
W
Cdt1
Cdt2

Fig6C

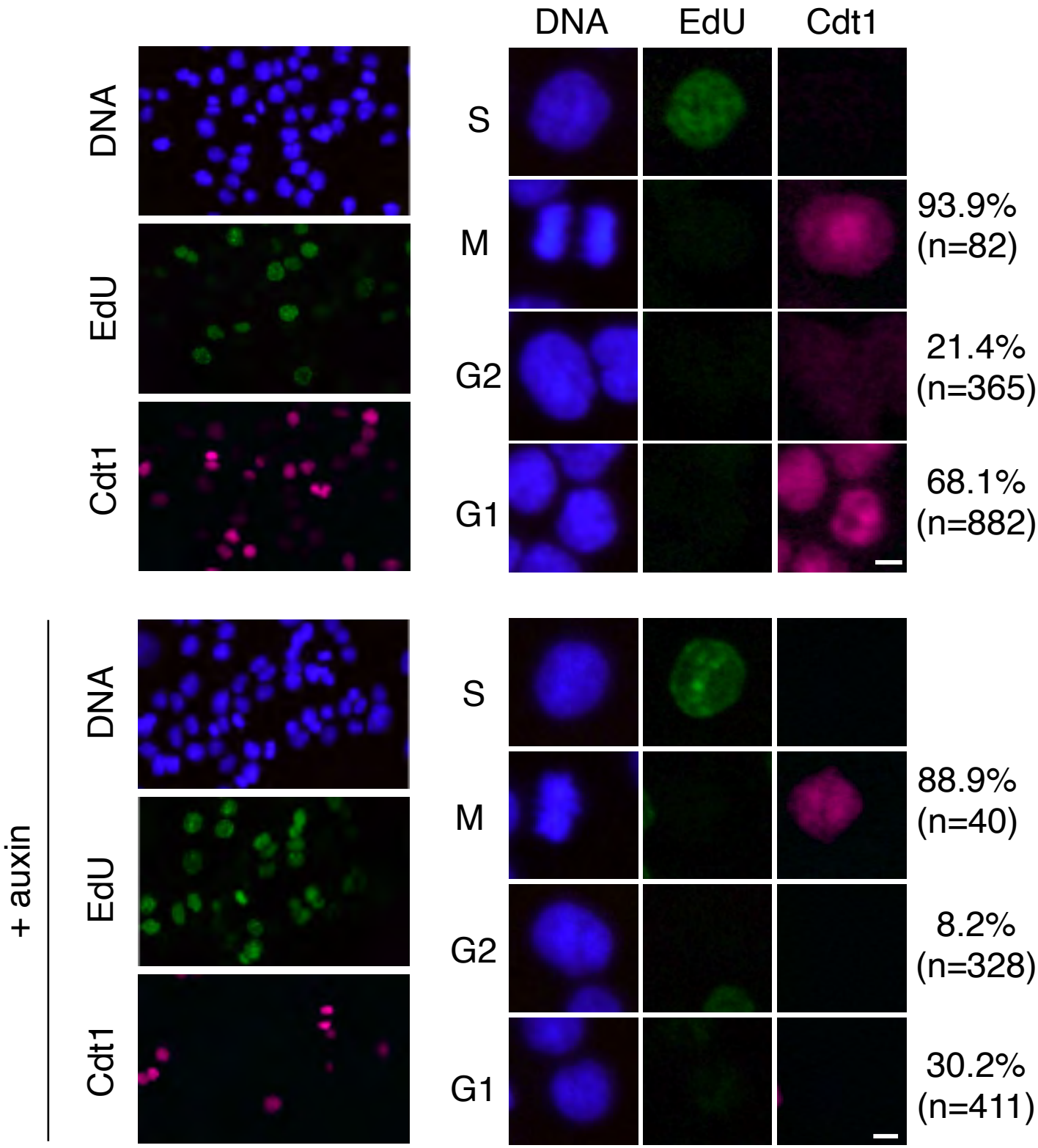
DNA
EdU
Cdt1
DNA
EdU
Cdt1
S
M
G2
G1
93.9%
(n=82)
21.4%
(n=365)
68.1%
(n=882)
+ auxin
DNA
EdU
Cdt1
S
M
G2
G1
88.9%
(n=40)
8.2%
(n=328)
30.2%
(n=411)